for ubiquitination assay instruction; and S. Sakiyama for reading the manuscript.

REFERENCES

1. Rosen, D. R., Siddique, T., Patterson, D., Figlewicz, D. A., Sapp, P., Hentati, A., Donaldson, D., Goto, J., O'Regan, J. P., Deng, H. X., Rahmani, Z., Krizus, A., McKenna-Yasek, D., Cayabyab, A., Gaston, S. M., Berger, R., Tanzi, R. E., Halperin, J. J., Herzfeldt, B., van den Bergh, R., Hung, W.-Y., Bird, T., Deng, G., Mulder, D. W., Smyth, C., Laing, N. G., Soriano, E., Pericak-Vance, M. A., Haines, J., Rouleau, G. A., Gusella, J. S., Horvitz, H. R., and Brown, R. H., Jr. (1993) *Nature* **364,** 59–62
2. Deng, H. X., Hentati, A., Tainer, J. A., Iqbal, Z., Cayabyab, A., Hung, W.-Y., Getzoff, E. D., Hu, P., Herzfeldt, B., Roos, R. P., Warner, C., Deng, G., Soriano, E., Smyth, C., Parge, H. E., Ahmed, A., Roses, A. D., Hallewell, R., Rericak-Vance, M. A., and Siddique, T. (1993) *Science* **261,** 1047–1051
3. Cleveland, D. W., and Liu, J. (2001) *Nat. Med.* **6,** 1320–1321
4. Brown, R. H., Jr., and Robberecht, W. (2001) *Semin. Neurol.* **21,** 131–139
5. Cluskey, S., and Ramsden, D. B. (2001) *Mol. Pathol.* **54,** 386–392
6. Orrell, R. W., and Figlewicz, D. A. (2001) *Neurology* **57,** 9–17
7. Keller, J. N., Huang, F. F., and Markesbery, W. R. (2000) *Neuroscience* **98,** 149–156
8. Hoffman, E. K., Wilcox, H. M., Scott, R. W., and Siman, R. (1996) *J. Neurol. Sci.* **139,** 15–20
9. Kunst, C. B., Mezey, E., Brownstein, M. J., and Patterson, D. (1997) *Nat. Genet.* **15,** 91–94
10. Hartmann, E., Gorlich, D., Kostka, S., Otto, A., Kraft, R., Knespel, S., Burger, E., Rapoport, T. A., and Prehn, S. (1993) *Eur. J. Biochem.* **214,** 375–381
11. Kato, S., Shimoda, M., Watanabe, Y., Nakashima, K., Takahashi, K., and Ohama, E. (1996) *J. Neuropathol. Exp. Neurol.* **55,** 1089–1101
12. Kato, S., Hayashi, H., Nakashima, K., Nanba, E., Kato, M., Hirano, A., Nakano, I., Asayama, K., and Ohama, E. (1997) *Am. J. Pathol.* **151,** 611–620
13. Nagai, M., Aoki, M., Miyoshi, I., Kato, M., Pasinelli, P., Kasai, N., Brown, R. H., Jr., and Itoyama, Y. (2001) *J. Neurosci.* **21,** 9246–9254
14. Nakagawara, A. (1998) *Med. Pediatr. Oncol.* **31,** 113–115
15. Harvey, K. F., and Kumar, S. (1999) *Trends Cell Biol.* **9,** 166–169
16. Kumar, S., Tomooka, Y., and Noda, M. (1992) *Biochem. Biophys. Res. Commun.* **30,** 1155–1161
17. Kato, S., Takikawa, M., Nakashima, K., Hirano, A., Cleveland, D. W., Kusaka, H., Shibata, N., Kato, M., Nakano, I., and Ohama, E. (2000) *Amyotroph. Lateral Scler. Other Motor Neuron Disord.* **1,** 163–184
18. Orrell, R. W. (2000) *Neuromuscul. Disord.* **10,** 63–68
19. Cudkowicz, M. E., McKenna-Yasek, D., Sapp, P. E., Chin, W., Geller, B., Hayden, D. L., Schoenfeld, D. A., Hosler, B. A., Horvitz, H. R., and Brown, R. H., Jr. (1997) *Ann. Neurol.* **41,** 210–221
20. Ratovitski, T., Corson, L. B., Strain, J., Wong, P., Cleveland, D. W., Culotta, V. C., and Borchelt, D. R. (1999) *Hum. Mol. Genet.* **8,** 1451–1460
21. Aoki, M., Ogasawara, M., Matsubara, Y., Narisawa, K., Nakamura, S., Itoyama, Y., and Abe, K. (1993) *Nat. Genet.* **5,** 323–324
22. Kato, M., Aoki, M., Ohta, M., Nagai, M., Ishizaki, F., Nakamura, S., and Itoyama, Y. (2001) *Neurosci. Lett.* **312,** 165–168
23. Andersen, P. M., Forsgren, L., Binzer, M., Nilsson, P., Ala-Hurula, V., Keranen, M. L., Bergmark, L., Saarinen, A., Haltia, T., Tarvainen, I., Kinnunen, E., Udd, B., and Marklund, S. L. (1996) *Brain* **119,** 1153–1172
24. Shibata, N., Hirano, A., Kobayashi, M., Siddique, T., Deng, H. X., Hung, W.-Y., Kato, T., and Asayama, K. (1996) *J. Neuropathol. Exp. Neurol.* **55,** 481–490
25. Sussman, D. J., Klingensmith, J., Salinas, P., Adams, P. S., Nusse, R., and Perrimon, N. (1994) *Dev. Biol.* **166,** 73–86
26. Wodarz, A., and Nusse, R. (1998) *Annu. Rev. Cell Dev. Biol.* **14,** 59–88
27. Boutros, M., Paricio, N., Strutt, D. I., and Mlodzik, M. (1998) *Cell* **94,** 109–118
28. Julien, J. P. (2001) *Cell* **104,** 581–591
29. Fons, R. D., Bogert, B. A., and Hegde, R. S. (2003) *J. Cell Biol.* **160,** 529–539
30. Fujita, Y., Okamoto, K., Sakurai, A., Gonatas, N. K., and Hirano, A. (2000) *J. Neurol. Sci.* **174,** 137–140
31. Mourelatos, Z., Gonatas, N. K., Stieber, A., Gurney, M. E., and Dal Canto, M. C. (1996) *Proc. Natl. Acad. Sci. U. S. A.* **93,** 5472–5477
32. Wharton, K. A., Jr. (2003) *Dev. Biol.* **253,** 1–17
33. Tsang, M., Lijam, N., Yang, Y., Beier, D. R., Wynshaw-Boris, A., and Sussman, D. J. (1996) *Dev. Dyn.* **207,** 253–262
34. Krylova, O., Messenger, M. J., and Salinas, P. C. (2000) *J. Cell Biol.* **151,** 83–94
35. Julien, J. P., and Beaulieu, J. M. (2000) *J. Neurol. Sci.* **180,** 7–14
36. Luo, Z. G., Wang, Q., Zhou, J. Z., Wang, J., Luo, Z., Liu, M., He, X., Wynshaw-Boris, A., Xiong, W. C., Lu, B., and Mei, L. (2002) *Neuron* **35,** 489–505
37. De Ferrari, G. V., and Inestrosa, N. C. (2000) *Brain Res. Brain Res. Rev.* **33,** 1–12
38. Kaytor, M. D., and Orr, H. T. (2000) *Curr. Opin. Neurobiol.* **12,** 275–278
39. Versteeg, R., Caron, H., Cheng, N. C., van der Drift, P., Slater, R., Westerveld, A., Voute, P. A., Delattre, O., Laureys, G., van Roy, N., and Speleman, F. (1995) *Eur. J. Cancer* **31,** 538–541
40. Murata, S., Minami, Y., Minami, M., Chiba, T., and Tanaka, K. (2001) *EMBO Rep.* **2,** 1133–1138
41. Okado-Matsumoto, A., and Fridovich, I. (2002) *Proc. Natl. Acad. Sci. U. S. A.* **99,** 9010–9014
42. Niwa, J., Ishigaki, S., Hishikawa, N., Yamamoto, M., Doyu, M., Murata, S., Tanaka, K., Taniguchi, N., and Sobue, G. (2002) *J. Biol. Chem.* **277,** 36793–36798
43. Mori, K. (2000) *Cell* **101,** 451–454
44. Travers, K. J., Patil, C. K., Wodicka, L., Lockhart, D. J., Weissman, J. S., and Walter, P. (2000) *Cell* **101,** 249–258
45. Wickner, S., Maurizi, M. R., and Gottesman, S. (1999) *Science* **286,** 1888–1893
46. Borchelt, D. R., Lee, M. K., Slunt, H. S., Guarnieri, M., Xu, Z. S., Wong, P. C., Brown, R. H., Jr., Price, D. L., Sisodia, S. S., and Cleveland, D. W. (1994) *Proc. Natl. Acad. Sci. U. S. A.* **16,** 8292–8296

Acta Neuropathol (2004) 107 : 149–158
DOI 10.1007/s00401-003-0791-1

REGULAR PAPER

Shinsuke Kato · Yusuke Saeki · Masashi Aoki · Makiko Nagai · Aya Ishigaki · Yasuto Itoyama · Masako Kato
Kohtaro Asayama · Akira Awaya · Asao Hirano · Eisaku Ohama

Histological evidence of redox system breakdown caused by superoxide dismutase 1 (SOD1) aggregation is common to SOD1-mutated motor neurons in humans and animal models

Received: 8 July 2003 / Revised: 10 October 2003 / Accepted: 13 October 2003 / Published online: 27 November 2003

Abstract Living cells produce reactive oxygen species (ROSs). To protect themselves from these ROSs, the cells have developed both an antioxidant system containing superoxide dismutase 1 (SOD1) and a redox system including peroxiredoxin2 (Prx2, thioredoxin peroxidase) and glutathione peroxidase1 (GPx1): SOD1 converts superoxide radicals into hydrogen peroxide (H_2O_2), and H_2O_2 is then converted into harmless water (H_2O) and oxygen (O_2) by Prx2 and GPx1 that directly regulate the redox system. To clarify the biological significance of the interaction of the redox system (Prx2/GPx1) with SOD1 in SOD1-mutated motor neurons in vivo, we produced an affinity-purified rabbit antibody against Prx2 and investigated the immunohistochemical localization of Prx2 and GPx1 in neuronal Lewy body-like hyaline inclusions (LBHIs) in the spinal cords of familial amyotrophic lateral sclerosis (FALS) patients with a two-base pair deletion at codon 126 and an Ala→Val substitution at codon 4 in the SOD1 gene, as well as in transgenic rats expressing human SOD1 with H46R and G93A mutations. The LBHIs in motor neurons from the SOD1-mutated FALS patients and transgenic rats showed identical immunoreactivities for Prx2 and GPx1: the reaction product deposits with the antibodies against Prx2 and GPx1 were localized in the LBHIs. In addition, the localizations of the immunoreactivities for SOD1 and Prx2/GPx1 were similar in the inclusions: the co-aggregation of Prx2/GPx1 with SOD1 in neuronal LBHIs in mutant SOD1-related FALS patients and transgenic rats was evident. Based on the fact that Prx2/GPx1 directly regulates the redox system, such co-aggregation of Prx2/GPx1 with SOD1 in neuronal LBHIs may lead to the breakdown of the redox system itself, thereby amplifying the mutant SOD1-mediated toxicity in mutant SOD1-linked FALS patients and transgenic rats expressing human mutant SOD1.

Keywords Peroxiredoxin 2 · Glutathione peroxidase 1 · Redox system · Superoxide dismutase 1 · Familial amyotrophic lateral sclerosis

S. Kato (✉) · Y. Saeki · E. Ohama
Department of Neuropathology,
Institute of Neurological Sciences, Faculty of Medicine,
Tottori University,
Nishi-cho 36-1, 683-8504 Yonago, Japan
Tel.: +81-859-348034, Fax: +81-859-348289,
e-mail: kato@grape.med.tottori-u.ac.jp

M. Aoki · M. Nagai · A. Ishigaki · Y. Itoyama
Department of Neuroscience, Division of Neurology,
Tohoku University Graduate School of Medicine, Sendai, Japan

M. Kato
Division of Pathology, Tottori University Hospital,
Yonago, Japan

K. Asayama
Department of Pediatrics,
University of Occupational and Environmental Health,
Kitakyushu, Japan

A. Awaya
Japan Science and Technology Corporation,
Tachikawa, Japan

A. Hirano
Division of Neuropathology,
Department of Pathology, Montefiore Medical Center,
Bronx, New York, USA

Introduction

Living cells produce reactive oxygen species (ROSs) during physiological processes and in response to external stimuli such as ultraviolet radiation. To protect itself from potentially destructive ROSs, each cell of living organisms has developed a sophisticated antioxidant enzyme defense system. In this system, there are two groups of enzymes: the enzymes of the first group convert superoxide radicals into hydrogen peroxide (H_2O_2), and the enzymes of the second group convert H_2O_2 into harmless water (H_2O) and oxygen (O_2). For the first antioxidant enzyme group, three isoforms of superoxide dismutase (SOD) [EC 1.15.1.1] have been identified: SOD1, SOD2, and SOD3 [9]. In the second enzyme group, the peroxiredoxin (Prx) and glutathione peroxidase (GPx) families, as well as catalase localized within peroxisomes have been identified. Unlike

SOD and catalase, enzymes of the Prx and GPx families require secondary enzymes and cofactors to function at high efficiency. In particular, the enzymes of the Prx- and GPx-families are considered to play a role in directly controlling the redox system. In general, the redox system regulates versatile control mechanisms in signal transduction and gene expression [29]. In mammalian cells, this redox signal transduction is linked to systems such as cellular differentiation, immune response, growth control, and apoptosis [10].

Peroxiredoxin2 (Prx2) is a novel organ-specific antioxidative enzyme that is mainly expressed in mammalian brain [23]. This protein is a member of Prx family, whose members possess reactive cysteine residues [23]. Prx2 requires thioredoxin reductase (TR) as a secondary enzyme as well as thioredoxin and NADPH as cofactors to function at high efficiency; the activity of Prx2 in the thioredoxin/TR/NADPH system is over five times higher than that of Prx2 by itself [5]. In this milieu, Prx2 is also called thioredoxin peroxidase 1 (thioredoxin-dependent peroxide reductase 1) or thiol-specific antioxidant [4, 5, 6]. In addition to controlling the intracellular content of H_2O_2, Prx2 directly regulates the redox signals of the thioredoxin/TR/NADPH system, because alone the secondary enzyme and cofactors (i.e., thioredoxin/TR/NADPH) can not directly regulate the redox system and can not act on H_2O_2. Cytosolic GPx [EC 1.11.1.9], a classical selenium-dependent isoform (also assigned as GPx1), was first described as an enzyme that protects hemoglobin from oxidative degradation in red blood cells [25]. The GPx family is composed of at least four GPx isoforms in mammals [7]. Among them, GPx1 is considered as the major enzyme responsible for removing intracytoplasmic H_2O_2. Like Prx2, GPx1 needs glutathione reductase (GR) as a secondary enzyme as well as glutathione and NADPH as cofactors to work at high efficiency, and this process is also one of the redox signals in living cells [21, 24]. Therefore, Prx2 and GPx1 directly control the redox system.

Approximately 20% of the cases of familial amyotrophic lateral sclerosis (FALS) are caused by a mutant SOD1 [15, 17, 18]. SOD1 is thought to be an essential component of neuronal Lewy body-like hyaline inclusions (LBHIs): neuronal LBHIs in affected anterior horn cells are morphological hallmarks of SOD1-mutated motor neurons of FALS patients [3, 11, 12, 13, 14, 15, 16, 17, 18, 30]. To cope with destructive ROSs, even SOD1-mutated motor neurons induce mutant and wild-type SOD1 as well as Prx2 and GPx1. Considering that Prx2 and GPx1 interact not only with wild-type SOD1 but also with mutant SOD1, the interaction of Prx2/GPx1 with SOD1 has been suggested to contribute to mutant SOD1 aggregation toxicity: Prx2/GPx1 possibly aggregate as LBHIs in SOD1-mutated motor neurons. Furthermore, the aggregation of Prx2/GPx1 might affect the intracytoplasmic redox regulation and amplify mutant SOD1-mediated toxicity. To clarify the biological significance of the interaction of Prx2/GPx1 (redox system) with SOD1 in SOD1-mutated motor neurons in vivo, we first produced an antibody against Prx2, and analyzed the characteristic expressions of both Prx2 and GPx1 in neuronal LBHIs in SOD1-mutated motor neurons of humans and animal models.

Materials and methods

Preparation of polyclonal antibody against Prx2

A synthetic peptide corresponding to the C-terminal region of Prx2 (amino acids 184–198: NH_2-KPNVDDSKEYFSKHN-COOH) with or without conjugation to human serum albumin (HSA) at the carboxyl end was supplied by Peptide Institute (Osaka, Japan). This amino acid sequence is homologous with those of the C-terminal region of the human, rat or mouse Prx2. The polyclonal antibody preparation was carried out according to the method of Kato et al. [16]. To prepare immunogen, 6 mg synthesized Prx2 peptide was conjugated with 6 mg keyhole limpet hemocyanin (KLH) in the presence of 50 mM 1-ethyl-3-(3-dimethylaminopropyl) carbodiimide-HCl (Pierce Chemical Co., Rockford, IL) and 2.5 mM *N*-hydroxysulfosuccinimide (Pierce) in 3 ml phosphate-buffered saline (PBS) pH 7.4 for 1 h at room temperature. The reaction was terminated by adding 2-mercaptoethanol to the concentration of 20 mM and dialyzed against PBS for 24 h. To raise polyclonal antibodies, 500 µg of the immunogen in 50% Freund's complete adjuvant was inoculated intradermally into a rabbit at 20 skin sites; four booster inoculations of 500 µg immunogen in 50% Freund's incomplete adjuvant were given at 10, 17, 24 and 31 days after the first inoculation. The serum was taken 10 days after the final immunization. The IgG fraction in the antiserum against the immunogen, the hapten-conjugated KLH, was purified by absorption on a protein G-Sepharose gel column (Pharmacia Biotech, Uppsala, Sweden). Subsequently, the antibodies were further purified on an affinity column of immobilized KLH conjugated with the synthetic Prx2 peptide, as described previously [16].

Enzyme-linked immunosorbent assay

Noncompetitive ELISA was carried out according to the method described by Kato et al. [16]. Each well of a 96-well microtiter plate was coated with 100 µl of 5 µg/ml immunogen in 5 mM sodium carbonate buffer (pH 9.6) and incubated for 60 min. This was followed by triplicate washing with PBS containing 0.05% Tween 20 (buffer A). Each well was blocked with 0.5% gelatin for 60 min and then washed three times with buffer A. Antibody solutions (100 µl) at the concentrations indicated in Fig. 1 (horizontal line) were added to each well and incubated for 60 min. The wells were then washed three times with buffer A. The binding of the horseradish peroxidase-conjugated secondary antibody (Wako Pure Chemical Industries, Osaka, Japan) to the primary antibody was visualized with 2, 2'-azino-bis-(3-ethylbenzothiazoline-6-sulfonate)-$(NH_3)_2$. The reaction was terminated with 1 M sulfuric acid, and the absorbance at 415 nm was read on a micro-ELISA plate reader (Tecan, Hombrechtikon, Switzerland).

Tissue collection

Histochemical and immunohistochemical studies were performed on archival, buffered 10% formalin-fixed, paraffin-embedded tissues obtained at autopsy from five FALS patients who were members of two different families. The main clinicopathological characteristics of the FALS patients are summarized in Table 1, and have been reported previously [12, 13, 20, 22, 28, 30, 31]. SOD1 analysis revealed that the members of the Japanese Oki family had a two-base pair deletion at codon 126 (frame-shift 126 mutation) [12] and the American C family members had an Ala→Val substitution at codon 4 (A4V) [30]. As human controls, we examined autopsy specimens of the spinal cord from 20 neurologically and neuropathologically normal individuals (11 male, 9 females; aged 37–75 years).

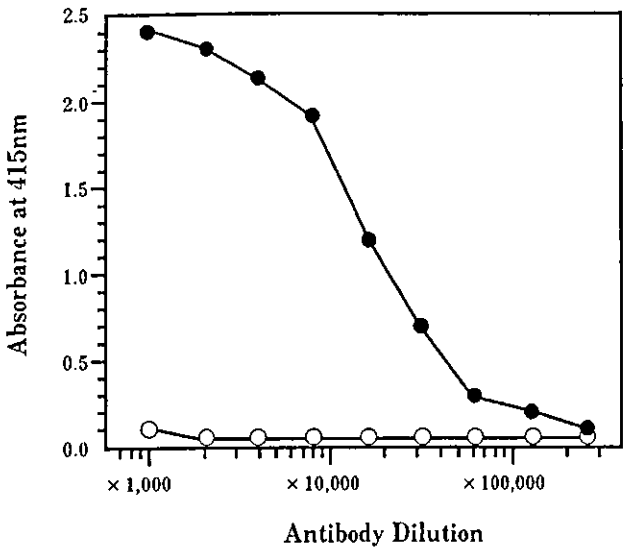

Fig. 1 Specificity of antibody against Prx2. The immunoreactivity of the antibody to HSA-conjugated Prx2 peptide (*solid circles*) and native HSA (*open circles*) was determined by noncompetitive ELISA. The anti-Prx2 antibody recognizes the HSA-conjugated Prx2 peptide, but does not react with HAS (*Prx2* peroxiredoxin2, *ELISA* enzyme-linked immunosorbent assay, *HAS* human serum albumin)

Histochemical and immunohistochemical studies were also carried out on specimens from transgenic rats with the H46R and G93A types of mutations (three rats of each type). The H46R rats used in this study were a transgenic line (H46R-4) in which the level of human SOD1 with the H46R mutation was 6 times the level of that of endogenous rat SOD1 [27]. The G93A rats were a transgenic line (G93A-39) in which the level of human SOD1 with the G93A mutation was 2.5 times the level of endogenous rat SOD1 [27]. These rats were killed at an age of over 180 days; an age corresponding to an advanced stage of disease in these strains. The detailed clinical signs and pathological characteristics of the neuronal LBHIs of the H46R and G93A rats have been demonstrated previously [27]. As rat controls, we investigated the spinal cord specimens of three age-matched littermates of H46R and G93A rats and five age-matched normal Sprague-Dawley rats. Rats were anesthetized with sodium pentobarbital (0.1 ml/100 g body weight). After perfusion of the rats via the aorta with physiological saline at 37°C, they were fixed by perfusion with 4% paraformaldehyde in 0.1 M cacodylate buffer (pH 7.3). The spinal cords were removed and then postfixed in the same solution.

Histochemistry and immunohistochemistry

After fixation, the specimens were embedded in paraffin, cut into 6-μm-thick sections, and examined by light microscopy. Spinal cord sections were stained by the following histochemical methods: hematoxylin and eosin (HE), Klüver-Barrera, Holzer, phosphotungstic acid-hematoxylin, periodic acid-Schiff, alcian blue, Masson's trichrome, Mallory azan and Gallyas-Braak stains. Representative paraffin sections were used for immunohistochemical assays. The following primary antibodies were utilized: an affinity-purified rabbit antibody against Prx2 (concentration: 1 μg/ml), a polyclonal antibody to GPx1 [diluted 1:2,000 in 1% bovine serum albumin-containing phosphate-buffered saline (BSA-PBS), pH 7.4] [2], and a polyclonal antibody to human SOD1 (diluted 1:10,000 in 1% BSA-PBS, pH 7.4) [1]. Sections were deparaffinized, and endogenous peroxidase activity was quenched by incubation for 30 min with 0.3% H_2O_2. The sections were then washed in PBS. Normal sera homologous with secondary antibody was used as a blocking reagent. Tissue sections were incubated with the primary antibodies for 18 h at 4°C. PBS-exposed sections served as controls. As a preabsorption test, some sections were incubated with the anti-Prx2 antibody that had been preabsorbed with an excess amount of the synthetic Prx2 peptide. Bound antibodies were visualized by the avidin-biotin-immunoperoxidase complex (ABC) method using the appropriate Vectastain ABC Kit (Vector Laboratories, Burlingame, CA) and 3,3'-diaminobenzidine tetrahydrochloride (DAB; Dako, Glostrup, Denmark) as chromogen.

Results

We successfully produced an affinity-purified rabbit antibody against Prx2 peptide (amino acids 184–198; although this amino acid sequence is homologous with that of each C-terminal region of the human, rat, mouse, Chinese hamster or Bos Taurus Prx2, this peptide does not share homology with other members of the Prx family or any other peptide sequence in GenomeNet), and applied it to stain of paraffin sections from both humans and rats. This anti-Prx2 antibody recognized the HSA-conjugated Prx2 peptide, but did not react with HSA (Fig. 1).

Analysis of the essential changes of five cases of FALS revealed a subtype of FALS with posterior column involvement (PCI). This subtype is characterized by the degeneration of the middle root zones of the posterior column, Clarke nuclei, and the posterior spinocerebellar tracts, in addition to spinal cord motor neuron lesions. A long-term surviving patient with a clinical course of 11 years

Table 1 Characteristics of five FALS cases (*FALS* familial amyotrophic lateral sclerosis, *SOD* superoxide dismutase, *LBHI* Lewy body-like hyaline inclusion, *2-bp* two-base pair, *PCI* posterior column involvement type, + detected, *ND* not determined, *As* asphyxia, *IH* intraperitoneal hemorrhage, *RD* respiratory distress, *Pn* pneumonia)

Case	Age (years)	Sex	Cause of Death	FALS Duration	SOD1 mutation	FALS subtype	Neuronal LBHI
Japanese Oki family							
1	46	F	As	18 months	2-bp deletion (126)	PCI	+
2	65	M	IH	11 years	2-bp deletion (126)	PCI and degeneration of other systems	+
American C family							
3	39	M	RD	7 months	A4V	PCI	+
4	46	M	Pn	8 months	A4V	PCI	+
5	66	M	Pn	1 year	ND	PCI	+

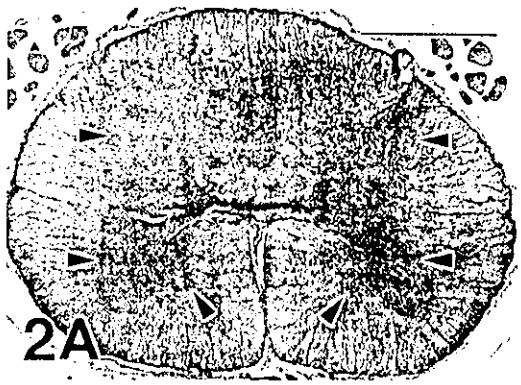
2A

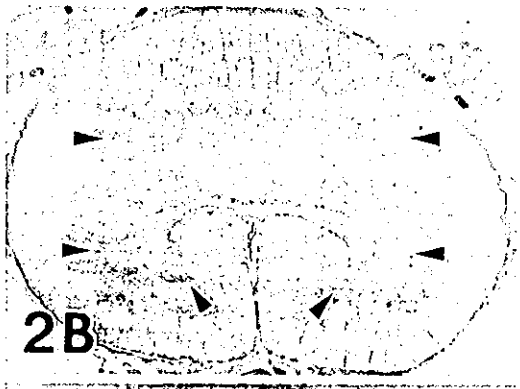
2B

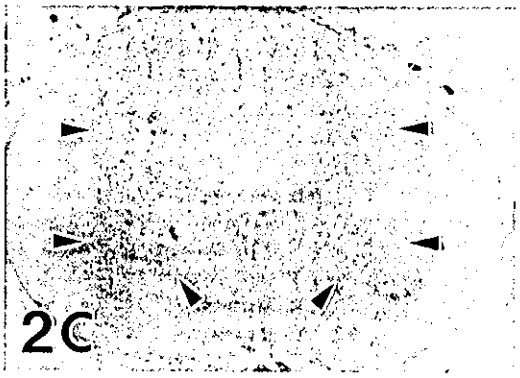
2C

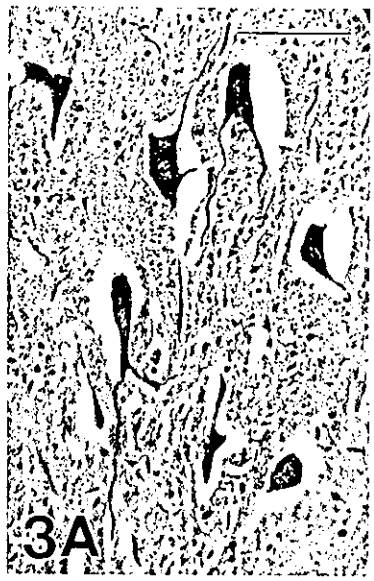
3A

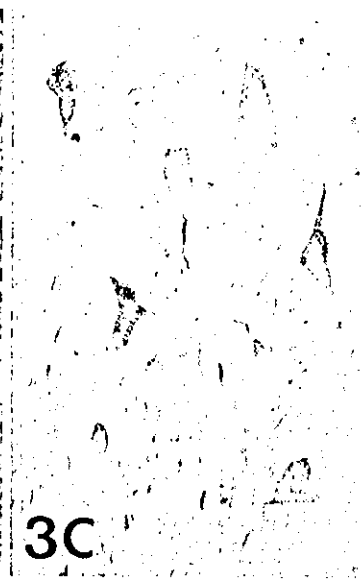
3C


3B


3D

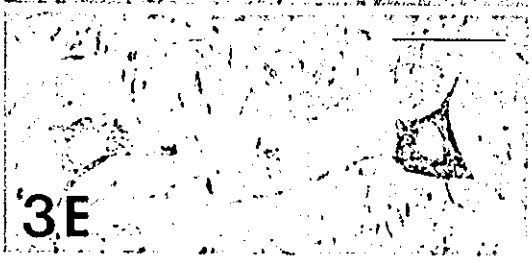
3E

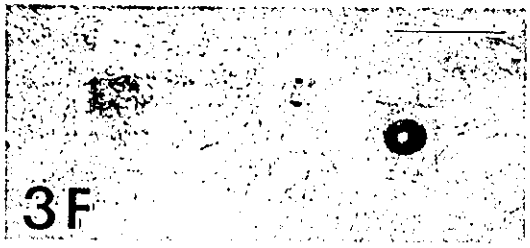
3F

◀ Fig. 2 Serial transverse sections through the lumbar segments of the normal human spinal cords. A Light microscopic preparation stained with HE. B, C Immunostaining for GPx1 (B) and Prx2 (C). GPx1 and Prx2 immunoreactivities are found diffusely in the neuropil with considerably less intensity (*arrowheads*). No counterstaining (*HE* hematoxylin and eosin, *GPx1* glutathione peroxidase1, *Prx2* peroxiredoxin2). *Bar* A (also for B, C) 2 mm

Fig. 3 Detection of Prx2 and GPx1 in the normal motor neurons of the human spinal cord. A–D Serial sections. A Staining with HE. B Immunostaining with the antibody against GPx1, showing GPx1-positive neurons. C Immunostaining with the antibody to Prx2. Immunoreactivity is identified in most of the neurons. Thus, most of the normal motor neurons in the spinal cord co-express both GPx1 (B) and Prx2 (C), although their staining intensities in neurons vary. D Immunostaining with anti-Prx2 antibody pretreated with an excess of the synthetic Prx2 peptide. No immunoreaction products are observed in the motor neurons and neuropil. E GPx1 immunostaining of the neuronal cytoplasm and proximal dendrites is observed, but no intranuclear localization is seen. F Prx2 immunostaining of the neuronal cytoplasm and proximal dendrites is observed, and a nucleus of the neuron is also immunostained by the anti-Prx2 antibody. B–F No counterstaining (*HE* hematoxylin and eosin, *GPx1* glutathione peroxidase1, *Prx2* peroxiredoxin2). *Bars* A (also for B–D) 100 μm; E, F 50 μm

(case 2 in Table 1) showed multisystem degeneration in addition to the features of FALS with PCI. Neuronal Lewy body-like hyaline inclusions (LBHIs) were present in all five FALS cases. As observed in HE preparations, the neuronal LBHIs in the FALS patients were essentially identical to those in the H46R and G93A transgenic rats; the inclusions were round eosinophilic or paler inclusions and often showed eosinophilic cores with pale peripheral halos. In mutant SOD1-linked FALS patients, the neuronal LBHIs were generally composed of eosinophilic cores with pale peripheral halos and sometimes showed ill-defined forms that consisted of obscure eosinophilic materials. In H46R and G93A transgenic rats, the intracytoplasmic LBHIs with cores and halos were less frequently observed and round or sausage-like LBHIs, which were though to be intradendritic LBHIs, were often seen in the neuropil, although these round or sausage-like LBHIs in the neuropil were not remarkable in the human FALS patients. Histochemically, most of the neuronal LBHIs in the H46R and G93A transgenic rats were argyrophilic in Gallyas-Braak stain, and they were generally blue to violet after Masson's trichrome or Mallory azan staining, similar to the histochemical findings of the neuronal LBHIs of the human FALS patients. The spinal cords of normal individuals in both humans and rats did not exhibit any distinct histopathological alterations.

When control and representative paraffin sections were incubated with PBS alone (i.e., no primary antibody), no staining was detected. Prx2 immunoreactivity in normal spinal cords was identified in almost all neurons. In addition, Prx2-immunostaining was found throughout the neuropil with considerably lower intensity (Fig. 2A, C). With respect to the intracellular localization of Prx2, immunostaining of the neuronal cytoplasm and proximal dendrites was specifically observed (Fig. 3A, C). Additionally, the nuclei of some neurons were immunostained by the anti-Prx2 antibody, albeit the staining of positively stained nuclei varied (Fig. 3F). Incubation of sections with anti-Prx2 antibody that had been pretreated with an excess of the synthetic Prx2 produced no staining (Fig. 3D).

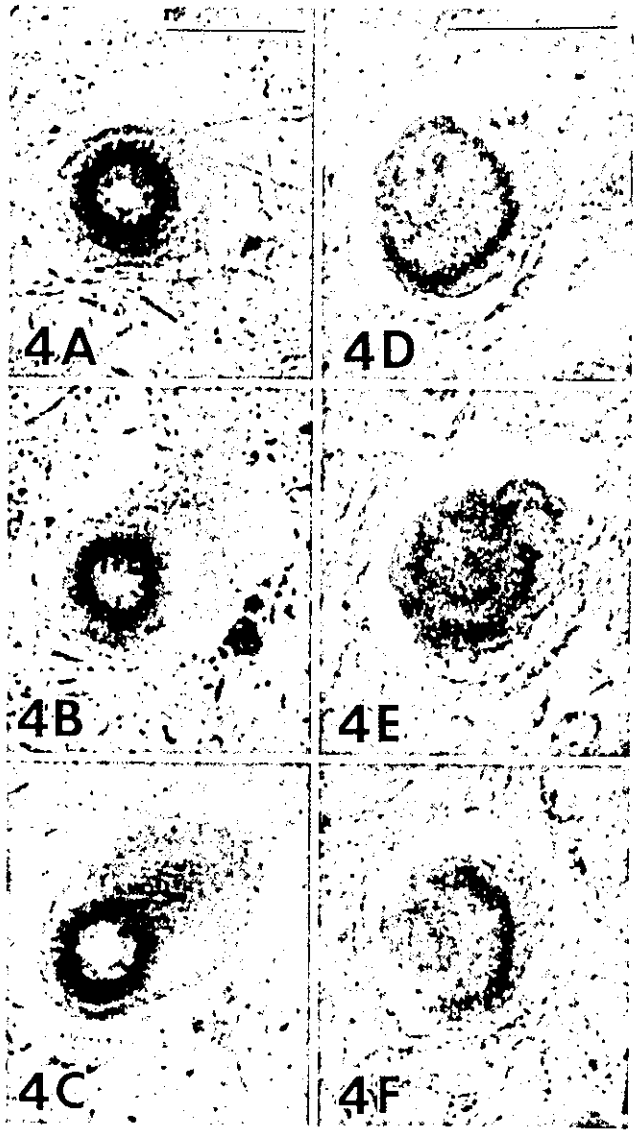

Fig. 4A–C Serial sections of a typical LBHI with a core and halo in neurons from the spinal cord of an FALS patient with a two-base pair deletion in the SOD1 gene. A Immunostaining for SOD1: immunoreactivity is mostly restricted to the halo. B Immunostaining for GPx1: immunoreactivity is located in the SOD1-positive portion of the LBHI. C Immunoreactivity for Prx2. Co-localization of the three proteins SOD1, GPx1 and Prx2 in the LBHI is evident. D–F Serial sections of a core and halo-type LBHI in a transgenic rat expressing human SOD1 with an H46R mutation. Immunostaining for SOD1 (D), GPx1 (E) and Prx2 (F). Similar stainability and immunolocalization of SOD1, GPx1 and Prx2 in the LBHI are observed (*LBHI* Lewy body-like hyaline inclusion, *FALS* familial amyotrophic lateral sclerosis, *SOD1* superoxide dismutase 1, *GPx1* glutathione peroxidase1, *Prx2* peroxiredoxin2). A–F No counterstaining. *Bars* A (also for B, C), D (also for E, F) 25 μm

A neuropil staining pattern similar to that for Prx2 was observed with GPx1; weak GPx1 immunoreactivity was diffusely seen in the neuropil in transverse sections of the

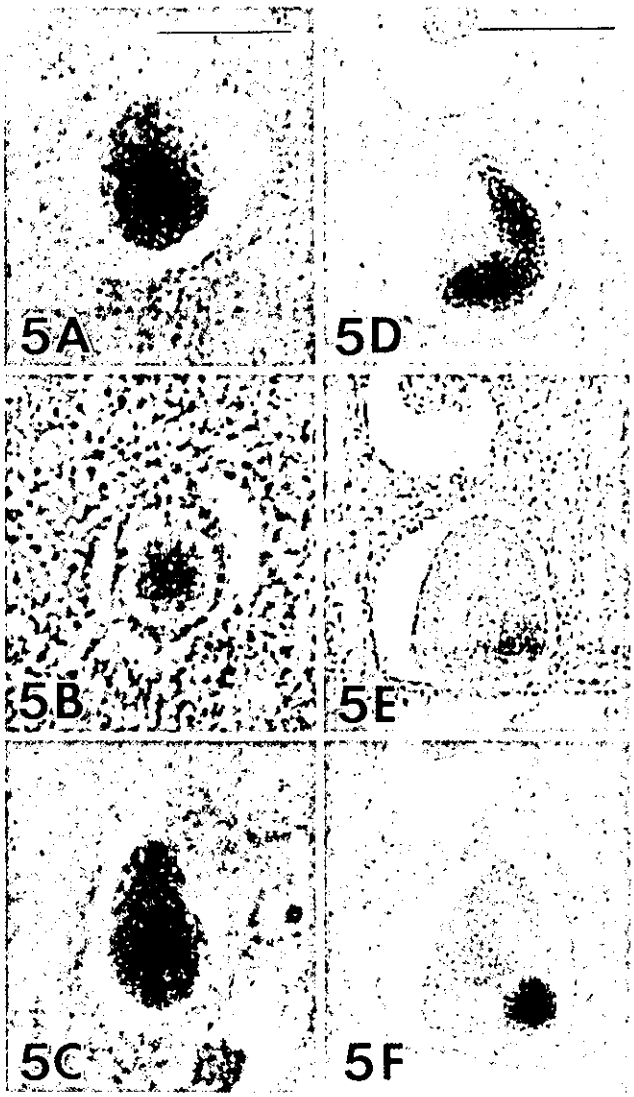

Fig. 5A–C Serial sections of an LBHI in an FALS patient with an A4V mutation in SOD1 gene. Immunostaining for SOD1 (A), GPx1 (B) and Prx2 (C). Co-localization of the three proteins in the LBHI is mainly observed in the core (A–C). D–F Serial sections of an LBHI in an FALS patient with a two-base pair deletion in the SOD1 gene. Immunostaining for SOD1 (D), GPx1 (E) and Prx2 (F). Immunostaining GPx1 (E) and Prx2 (F) are observed in only part of the SOD1-positive LBHI. The precise intra-inclusional immunolocalizations of these three proteins differ from each other in this LBHI (*LBHI* Lewy body-like hyaline inclusion, *FALS* familial amyotrophic lateral sclerosis, *SOD1* superoxide dismutase 1, *GPx1* glutathione peroxidase1, *Prx2* peroxiredoxin2). *Bars* A (also for B, C), D (also for E, F) 25 μm

spinal cords (Fig. 2A, B). GPx1 immunostaining was observed in the cytoplasm with cell bodies and proximal dendrites being essentially identified (Fig. 3A, B, E), but no intranuclear staining was observed (Fig. 3B, E). The stainability and intensity of Prx2 and GPx1 in the normal anterior horn cells of the spinal cords in humans were identical to those in rats. Therefore, almost all of the normal motor neurons in the spinal cords co-expressed both Prx2 and GPx1 (Fig. 3A–C), although the staining intensities of positively stained neurons varied.

Corroborating recent findings [12, 13, 16, 19, 27, 30], almost all of the neuronal LBHIs in both the FALS patients from two different families and races (Japanese Oki family and American C family) and the transgenic rats expressing two different human SOD1 mutations (H46R and G93A) were intensely immunostained by the antibody against human SOD1 (Figs. 4A, D; 5A, D; 6A; 7A). Most neuronal LBHIs were also immunoreactive for Prx2, although the intensity of Prx2 immunoreactivity in the LBHIs varied (Figs. 4C, F; 5C, F; 6B). The LBHIs in the neurons of the FALS patients and transgenic rats (H46R and G93A) showed a similar immunoreactivity for Prx2. The Prx2 immunolocalization in many intracytoplasmic and intraneuritic LBHIs was similar to that of SOD1 in both diseases. In core and halo-type LBHIs, the reaction product deposits of the antibody against Prx2 were generally restricted to the periphery (Fig. 4C, F), and were sometimes localized in the cores alone (Fig. 5C). In ill-defined LBHIs, Prx2 immunostaining was distributed throughout each inclusion. In some inclusions, however, expression of Prx2 was observed in only part of the inclusion (Fig. 5F). With respect to the GPx1 immunostaining in the neuronal LBHIs, similar stainability and immunolocalization to Prx2 were confirmed in the core and halo types as well as the ill-defined forms; most LBHIs in neurons were immunostained by the anti-GPx1 antibody with various intensities (Figs. 4B, E; 5B, E; 7B). The immunoreactivity for GPx1 in the FALS patients was similar to that in the transgenic rats (H46R and G93A). Like Prx2, the immunolocalization of GPx1 was similar to that of SOD1 in both diseases. GPx1-immunoreactive products in many core and halo-type inclusions were mainly localized in the periphery portions (Fig. 4B, E), but sometimes in the core portions alone (Fig. 5B). In some inclusions, the reaction products were confined to certain regions of each inclusion (Fig. 5E).

Noticeably, the co-localization of the three proteins SOD1, Prx2 and GPx1 in neuronal LBHIs in SOD1-mutated FALS patients and transgenic rats (H46R and G93A) was evident (Figs. 4, 5, 6, 7), although all three immunoreactive intensities varied. With respect to the intra-inclusional localization, many inclusions showed similar co-localizations of these three proteins (Figs. 4, 5A–C). In some LBHIs, the precise intra-inclusional immunolocalizations of the three proteins differed: Prx2 (Fig. 5D, F) and GPx1 (Fig. 5D, E) immunostaining was observed in only some areas of the SOD1-positive LBHIs.

Discussion

Under normal physiological conditions, Prx2 and GPx1 immunoreactivities in the spinal cord anterior horns in humans and rats are primarily identified in the neurons: cytoplasmic staining with both antibodies is observed in almost all of the anterior horn cells. Like Prx1 [26, 33], intranuclear localization in some neurons is also observed in Prx2 immunostaining. Considering that endogenous Prx2

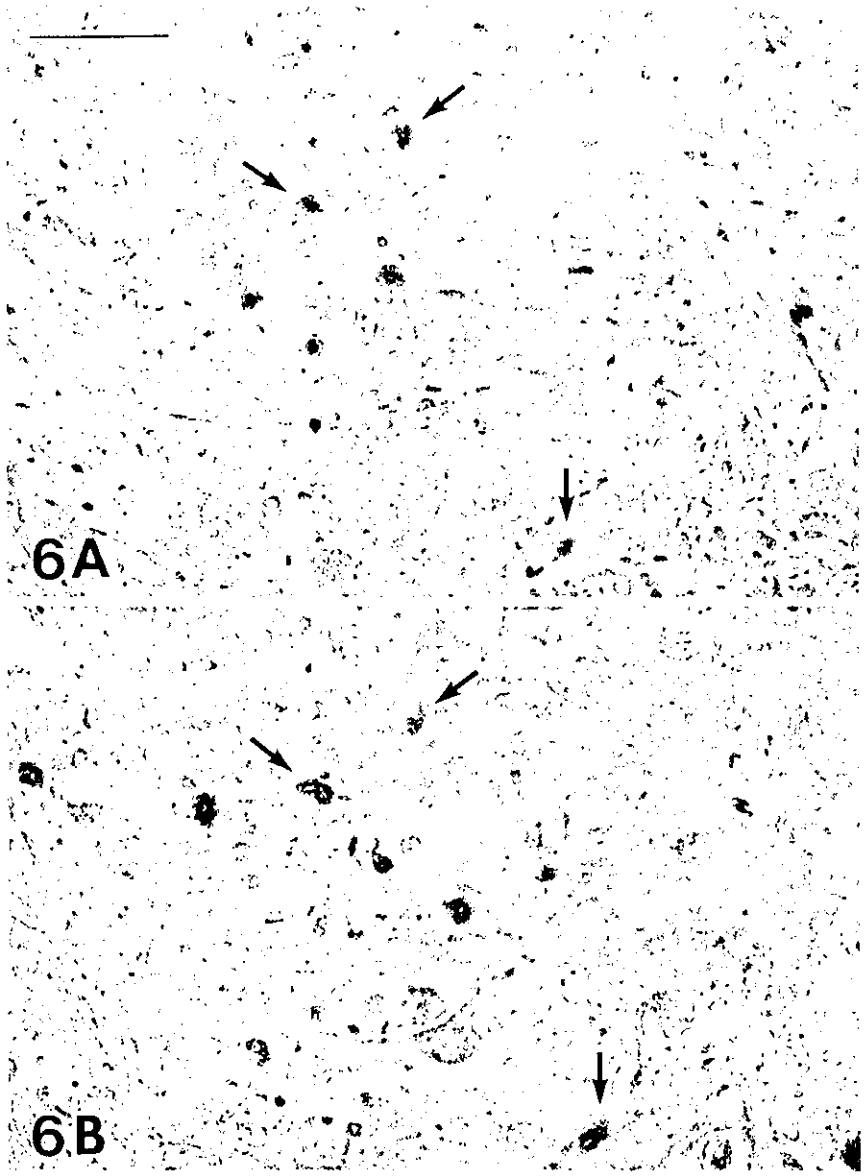

Fig. 6 Serial sections of the spinal anterior horn in a transgenic rat expressing human SOD1 with an H46R mutation immunostained with antibodies against SOD1 (A) and Prx2 (B). Round and sausage-like LBHIs in the neuropil are positive for both SOD1 and Prx2 (*arrows*) (*SOD1* superoxide dismutase1, *LBHI* Lewy body-like hyaline inclusion, *Prx2* peroxiredoxin2). *Bar* A (also for B) 50 μm

and GPx1 within the neuronal cytoplasm are extremely effective regulators of the redox system, our immunohistochemical finding that almost all of the normal spinal motor neurons co-expressed both Prx2 and GPx1 confirms that these motor neurons maintain themselves using the intracellular Prx2/GPx1 system, that is, the redox system.

As expected [12, 13, 16, 27, 30], SOD1 protein (probably the mutant form) was found to aggregate in the anterior horn cells as neuronal LBHIs in FALS patients with SOD1 gene mutations and transgenic rats expressing human SOD1 with H46R and G93A mutations. Intense co-expression of SOD1, Prx2, and GPx1 in neuronal LBHIs in both diseases was evident. To eliminate ROSs, SOD1-mutated motor neurons in mutant SOD1-linked FALS and transgenic rats (G46R and G93A) induce mutant/wild-type SOD1 as an antioxidant system and Prx2/GPx1 as a redox system. In this in vivo milieu where mutant SOD1 exists, Prx2 and GPx1 would aberrantly interact with the mutant SOD1, which is assumed to aggregate easily by itself [8]. Among the multiple theories of how mutant SOD1 contributes to motor neuron death in mutant SOD1-related FALS and transgenic animal models expressing human mutant SOD1, the aggregation of mutant SOD1 in neurons leads to part of the mutant SOD1-mediated toxicity through the formation of advanced glycation endproduct-modified SOD1 that is insoluble and cytotoxic [16]. Our recent study of FALS patients with a two-base pair deletion at codon 126 of the SOD1 gene (Oki family) and G85R transgenic mice has revealed that not only does mutant SOD1 provoke inclusion formation, but that normal SOD1 also co-aggregates in these inclusions [3]. Together with the facts that there are neuronal LBHIs positive for

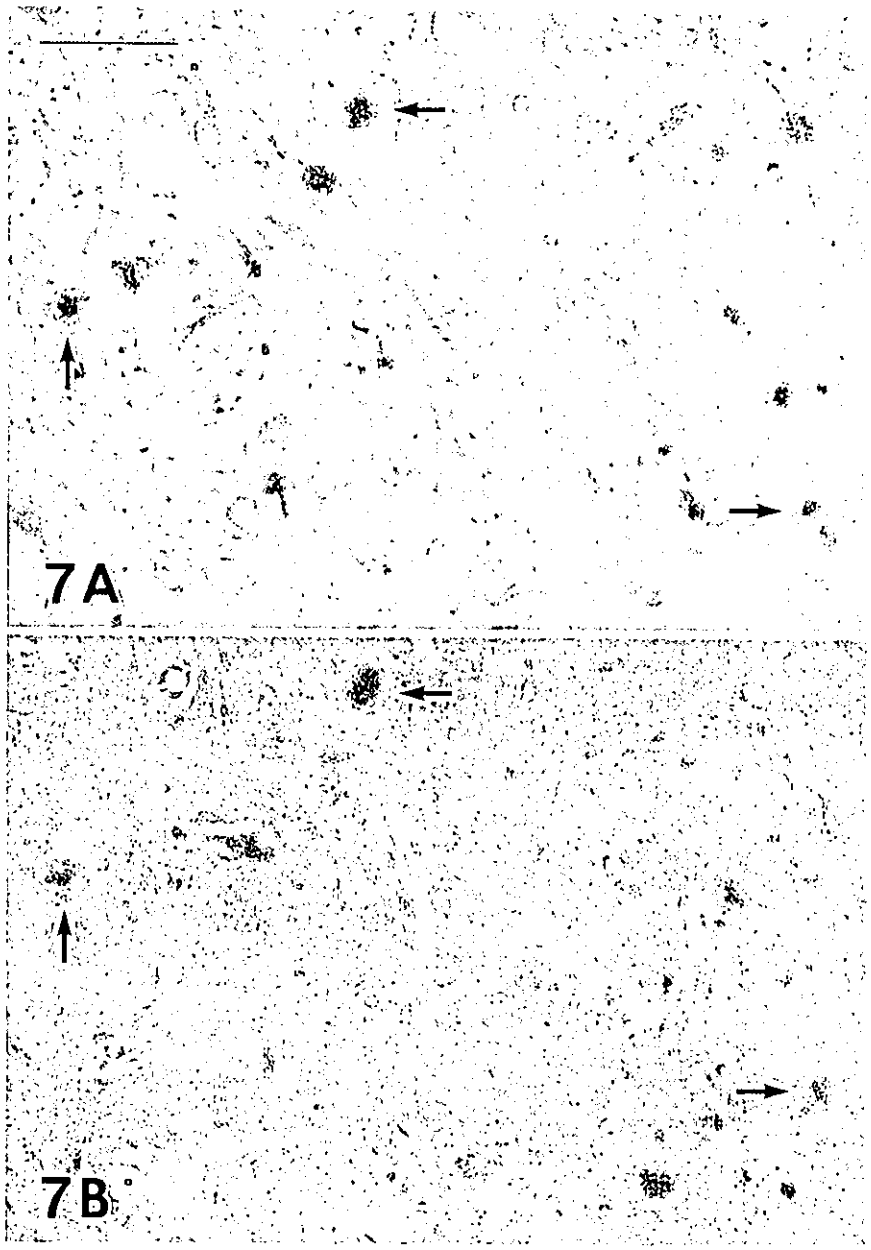

Fig. 7 Serial sections of the spinal anterior horn in a transgenic rat expressing human SOD1 with an H46R mutation immunostained with antibodies against SOD1 (A) and GPx1 (B). Round LBHIs in the neuropil are positive for both SOD1 and GPx1 (*arrows*) (*SOD1* superoxide dismutase1, *LBHI* Lewy body-like hyaline inclusion, *GPx1* glutathione peroxidase1). *Bar* A (also for B) 50 μm

SOD1, Prx2, and GPx1 in the milieu where mutant SOD1 exists but no LBHIs (no aggregations) exist under physiological conditions, our study demonstrates an aberrant interaction of Prx2/GPx1 with mutant SOD1, the aggregation of which results in neuronal LBHIs. In addition, intra-inclusional co-aggregation of Prx2/GPx1 with mutant SOD1 causes the intracytoplasmic reduction of Prx2/GPx1, thereby reducing the availability of the redox system. A similar aberrant interaction of the copper chaperone for SOD (CCS) and SOD1 (probably CCS-mutant SOD1) also occurs in the formation of the neuronal LBHIs in mutant SOD1-linked FALS [19] and the mutant SOD1 transgenic mouse model [32]. Such sequestration into LBHIs has also been observed for normal cytosolic constitutive proteins including tubulin and tau protein, as well as neuron-specific constitutive proteins containing phosphorylated neurofilament proteins (NFP), nonphosphorylated NFP, synaptophysin, and neuron-specific enolase [13, 17, 18]; this results in partial impairment of the maintenance of cell metabolism [13, 17, 18]. Although we cannot readily compare the sequestration of normal constitutive proteins with the aberrant interaction of cytotoxic mutant SOD1 with Prx2/GPx1 directly regulating a redox system, our finding leads us to speculate that not only co-aggregation of Prx2/GPx1 and SOD1 into LBHIs, but also intracytoplasmic reduction of Prx2/GPx1 in both diseases may partly contribute to the breakdown of the redox system itself in these SOD1-mutated neurons, and this may be one of the

endogenous mechanisms that accelerate neuronal death. This hypothesis would appear to be compatible with the aggregation toxicity theory. It remains to be determined whether this aberrant interaction of Prx2/GPx1 with mutant SOD1 is a direct or an indirect effect based on the pathogenesis of SOD1-mutated FALS disease itself or whether Prx2 and GPx1 play a primary or a secondary role to mutant SOD1. Consequently, we would like to emphasize that the aberrant interaction and co-aggregation of Prx2/GPx1 and SOD1 (probably Prx2/GPx1 and mutant SOD1) in FALS patients with SOD1 gene mutations and transgenic rats expressing human SOD1 mutations may amplify a more marked mutant SOD1-mediated toxicity.

Acknowledgements This study was supported in part by a Grant-in-Aid for Scientific Research (c) (2) from the Ministry of Education, Culture, Sports, Science and Technology of Japan (S.K.: 13680821) and by a Grant from the Ministry of Health, Labour and Welfare of Japan (S.K. and Y.I.).

References

1. Asayama K, Burr IM (1984) Joint purification of mangano and cuprozinc superoxide dismutases from a single source: a simplified method. Anal Biochem 136:336–339
2. Asayama K, Yokota S, Dobashi K, Hayashibe H, Kawaoi A, Nakazawa S (1994) Purification and immunoelectron microscopic localization of cellular glutathion peroxidase in rat hepatocytes: quantitative analysis by postembedding method. Histochemistry 102:213–219
3. Bruijn LI, Houseweart MK, Kato S, Anderson KL, Anderson SD, Ohama E, Reaume AG, Scott RW, Cleveland DW (1998) Aggregation and motor neuron toxicity of an ALS-linked SOD1 mutant independent from wild-type SOD1. Science 281: 1851–1854
4. Chae HZ, Kim IH, Kim K, Rhee SG (1993) Cloning, sequencing, and mutation of thiol-specific antioxidant gene of *Saccharomyces cerevisiae*. J Biol Chem 268:16815–16821
5. Chae HZ, Chung SJ, Rhee SG (1994) Thioredoxin-dependent peroxide reductase from yeast. J Biol Chem 269:27670–27678
6. Chae HZ, Robison K, Poole LB, Church G, Storz G, Rhee SG (1994) Cloning and sequencing of thiol-specific antioxidant from mammalian brain: alkyl hydroperoxide reductase and thiol-specific antioxidant define a large family of antioxidant enzymes. Proc Natl Acad Sci USA 91:7017–7021
7. De Haan JB, Bladier C, Griffiths P, Kelner M, O'Shea RD, Cheung NS, Bronson RT, Silvestro MJ, Wild S, Zheng SS, Beart PM, Hertzog PJ, Kola I (1998) Mice with a homozygous null mutation for the most abundant glutathione peroxidase, Gpx1, show increased susceptibility to the oxidative stress-inducing agents paraquat and hydrogen peroxide. J Biol Chem 273:22528–22536
8. Durham HD, Roy J, Dong L, Figlewicz DA (1997) Aggregation of mutant Cu/Zn superoxide dismutase proteins in a culture model of ALS. J Neuropathol Exp Neurol 56:523–530
9. Fridovich I (1986) Superoxide dismutases. Adv Enzymol Relat Area Mol Biol 58:61–97
10. Jin D-Y, Chae HZ, Rhee SG, Jeang K-T (1997) Regulatory role for a novel human thioredoxin peroxidase in NF-kappaB activation. J Biol Chem 272:30952–30961
11. Kato S, Shimoda M, Morita T, Watanabe Y, Nakashima K, Takahashi K, Ohama E (1996) Neuropathology of familial ALS with a mutation of the superoxide dismutase 1 gene. In: Nakano I, Hirano A (eds) Amyotrophic lateral sclerosis: progress and perspectives in basic research and clinical application. Elsevier Science, Amsterdam, pp 117–122
12. Kato S, Shimoda M, Watanabe Y, Nakashima K, Takahashi K, Ohama E (1996) Familial amyotrophic lateral sclerosis with a two base pair deletion in superoxide dismutase 1 gene: multisystem degeneration with intracytoplasmic hyaline inclusions in astrocytes. J Neuropathol Exp Neurol 55:1089–1101
13. Kato S, Hayashi H, Nakashima K, Nanba E, Kato M, Hirano A, Nakano I, Asayama K, Ohama E (1997) Pathological characterization of astrocytic hyaline inclusions in familial amyotrophic lateral sclerosis. Am J Pathol 151:611–620
14. Kato S, Horiuchi S, Nakashima K, Hirano A, Shibata N, Nakano I, Saito M, Kato M, Asayama K, Ohama E (1999) Astrocytic hyaline inclusions contain advanced glycation endproducts in familial amyotrophic lateral sclerosis with superoxide dismutase 1 gene mutation: immunohistochemical and immunoelectron microscopical analyses. Acta Neuropathol 97: 260–266
15. Kato S, Saito M, Hirano A, Ohama E (1999) Recent advances in research on neuropathological aspects of familial amyotrophic lateral sclerosis with superoxide dismutase 1 gene mutations: neuronal Lewy body-like hyaline inclusions and astrocytic hyaline inclusions. Histol Histopathol 14:973–989
16. Kato S, Horiuchi S, Liu J, Cleveland DW, Shibata N, Nakashima K, Nagai R, Hirano A, Takikawa M, Kato M, Nakano I, Ohama E (2000) Advanced glycation endproduct-modified superoxide dismutase-1 (SOD1)-positive inclusions are common to familial amyotrophic lateral sclerosis patients with SOD1 gene mutations and transgenic mice expressing human SOD1 with G85R mutation. Acta Neuropathol 100:490–505
17. Kato S, Takikawa M, Nakashima K, Hirano A, Cleveland DW, Kusaka H, Shibata N, Kato M, Nakano I, Ohama E (2000) New consensus research on neuropathological aspects of familial amyotrophic lateral sclerosis with superoxide dismutase 1 (SOD1) gene mutations: inclusions containing SOD1 in neurons and astrocytes. Amyotroph Lateral Scler Other Motor Neuron Disord 1:163–184
18. Kato S, Nakashima K, Horiuchi S, Nagai R, Cleveland DW, Liu J, Hirano A, Takikawa M, Kato M, Nakano I, Sakoda S, Asayama K, Ohama E (2001) Formation of advanced glycation end-product-modified superoxide dismutase-1 (SOD1) is one of the mechanisms responsible for inclusions common to familial amyotrophic lateral sclerosis patients with SOD1 gene mutation, and transgenic mice expressing human SOD1 gene mutation. Neuropathology 21:67–81
19. Kato S, Sumi-Akamaru H, Fujimura H, Sakoda S, Kato M, Hirano A, Takikawa M, Ohama E (2001) Copper chaperone for superoxide dismutase co-aggregates with superoxide dismutase 1 (SOD1) in neuronal Lewy body-like hyaline inclusions: an immunohistochemical study on familial amyotrophic lateral sclerosis with SOD1 gene mutation. Acta Neuropathol 102:233–238
20. Kato T, Hirano A, Kurland LT (1987) Asymmetric involvement of the spinal cord involving both large and small anterior horn cells in a case of familial amyotrophic lateral sclerosis. Clin Neuropathol 6:67–70
21. Kosower NS, Kosower EM (1978) The glutathione status of cells. Int Rev Cytol 54:109–160
22. Kurland LT, Mulder DW (1955) Epidemiologic investigations of amyotrophic lateral sclerosis. II. Familial aggregations indicative of dominant inheritance. Neurology 5:249–268
23. Matsumoto A, Okado A, Fujii T, Fujii J, Egashira M, Niikawa N, Taniguchi N (1999) Cloning of the peroxiredoxin gene family in rats and characterization of the fourth member. FEBS Lett 443:246–250
24. Meister A, Anderson ME (1983) Glutathione. Annu Rev Biochem 52:711–760
25. Mills GC (1957) Hemoglobin catabolism. 1. Glutathione peroxidase, an erythrocyte enzyme which protects hemoglobin from oxidative breakdown. J Biol Chem 229:189–197
26. Mu ZM, Yin XY, Prochownik EV (2002) Pag, a putative tumor suppressor, interacts with the Myc Box II domain of c-Myc and selectively alters its biological function and target gene expression. J Biol Chem 277:43175–43184

27. Nagai M, Aoki M, Miyoshi I, Kato M, Pasinelli P, Kasai N, Brown RH Jr, Itoyama Y (2001) Rats expressing human cytosolic copper-zinc superoxide dismutase transgenes with amyotrophic lateral sclerosis: associated mutations develop motor neuron disease. J Neurosci 21:9246–9254
28. Nakano I, Hirano A, Kurland LT, Mulder DW, Holley PW, Saccomanno G (1984) Familial amyotrophic lateral sclerosis. Neuropathology of two brothers in American "C" family. Neurol Med (Tokyo) 20:458–471
29. Sen CK, Packer L (1996) Antioxidant and redox regulation of gene transcription. FASEB J 10:709–720
30. Shibata N, Hirano A, Kobayashi M, Siddique T, Deng HX, Hung WY, Kato T, Asayama K (1996) Intense superoxide dismutase-1 immunoreactivity in intracytoplasmic hyaline inclusions of familial amyotrophic lateral sclerosis with posterior column involvement. J Neuropathol Exp Neurol 55:481–490
31. Takahashi K, Nakamura H, Okada E (1972) Hereditary amyotrophic lateral sclerosis. Histochemical and electron microscopic study of hyaline inclusions in motor neurons. Arch Neurol 27:292–299
32. Watanabe M, Dykes-Hoberg M, Culotta VC, Price DL, Wong PC, Rothstein JD (2001) Histological evidence of protein aggregation in mutant SOD1 transgenic mice and in amyotrophic lateral sclerosis neural tissues. Neurobiol Dis 8:933–941
33. Wen ST, Van Etten RA (1997) The PAG gene product, a stress-induced protein with antioxidant properties, is an Abl SH3-binding protein and a physiological inhibitor of c-Abl tyrosine kinase activity. Genes Dev 11:2456–2467

THE JOURNAL OF BIOLOGICAL CHEMISTRY
Vol. 280, No. 6, Issue of February 11, pp. 5061–5070, 2005
Printed in U.S.A.

Different Immunoreactivity against Monoclonal Antibodies between Wild-type and Mutant Copper/Zinc Superoxide Dismutase Linked to Amyotrophic Lateral Sclerosis*

Received for publication, June 2, 2004, and in revised form, October 29, 2004
Published, JBC Papers in Press, November 2, 2004, DOI 10.1074/jbc.M406106200

Noriko Fujiwara‡, Yasuhide Miyamoto§, Kyoko Ogasahara¶, Motoko Takahashi§, Takahisa Ikegami¶, Rina Takamiya§, Keiichiro Suzuki‡, and Naoyuki Taniguchi§||

From the ‡Department of Biochemistry, Hyogo College of Medicine, 1-1 Mukogawa-cho, Nishinomiya, Hyogo 663-8501, the §Department of Biochemistry, Osaka University Medical School & Graduate School of Medicine, 2-2 Yamadaoka, Suita, Osaka 565-0871, and ¶Institute of Protein Research, Osaka University, 3-2 Yamadaoka, Suita, Osaka 565-0871, Japan

Although more than 100 mutations have been identified in the copper/zinc superoxide dismutase (Cu/Zn-SOD) in familial amyotrophic lateral sclerosis (FALS), the mechanism responsible for FALS remains unclear. The finding of the present study shows that FALS-causing mutant Cu/Zn-SOD proteins (FALS mutant SODs), but not wild-type SOD, are barely detected by three monoclonal antibodies (mAbs) in Western blot analyses. The enzyme-linked immunosorbent assay for denatured FALS mutant SODs by dithiothreitol, SDS, or heat treatment also showed a lowered immunoreactivity against the mAbs compared with wild-type SOD. Because all the epitopes of these mAbs are mapped within the Greek key loop (residues 102–115 in human Cu/Zn-SOD), these data suggest that different conformational changes occur in the loop between wild-type and FALS mutant SODs during the unfolding process. Circular dichroism measurements revealed that the FALS mutant SODs are sensitive to denaturation by dithiothreitol, SDS, or heat treatment, but these results do not completely explain the different recognition by the mAbs between wild-type and FALS mutant SODs under the denatured conditions. The study on the conformational changes in local areas monitoring with mAbs may provide a new insight into the etiology of FALS.

Amyotrophic lateral sclerosis (ALS)[1] is a neurological disease characterized by selective motor neurons in the brain and spinal cord. Although most reported cases are sporadic ALS, 5–10% are familial ALS (FALS). About 20–25% of FALS cases have been shown to be associated with mutations in the copper/zinc superoxide dismutase (Cu/Zn-SOD) gene, *SOD1* on chromosome 21q22.1 (1, 2). Cu/Zn-SOD is a homodimer containing one copper ion and one zinc ion in each 16-kDa subunit. Cu/Zn-SOD catalyzes the disproportionation of superoxide anion (O_2^-) into O_2 and H_2O_2 and has been shown to play a protective role in cells against oxidative stress. To date, more than 100 FALS-causing mutations in the Cu/Zn-SOD, which consists of 153 amino acids, have been identified (3). Although some FALS causing-mutant Cu/Zn-SOD proteins (FALS mutant SODs) show less enzymatic activities, many retain full activity (4). Several lines of transgenic mice that express mutant human *SOD1* linked with FALS developed progressive neurodegeneration and a phenotype that clearly resembles human FALS (5, 6) despite having higher SOD activity. In contrast, *SOD1*-knock out mice do not exhibit motor neuron dysfunction (7). These findings suggest that this disease is the result of a toxic gain of function but not a loss in SOD activity. Several different hypotheses have been proposed to explain the toxic gain of function, including the production of ROS, mitochondrial defects, glutamate-induced excitotoxicity, neurofilament inclusions, and the formation of intracellular toxic protein aggregates (reviewed in Ref. 8). However, the mechanism by which FALS mutant SODs causes motor neuron degeneration is not completely understood.

The tertiary structure of Cu/Zn-SOD is characterized by the presence of a Greek key β-barrel containing an internal disulfide bond between Cys-57 and Cys-146 (9, 10), both of which contribute to its high stability. On the other hand, various FALS mutant SODs show a decreased stability and a lower level of metallation (4, 11, 12). Several reports, including ours (Fig. 1),[2] reported that FALS mutant SODs exhibit an accelerated turnover or an increased susceptibility to degradation in proteasome (13, 14) and suggest that unfolding or conformational perturbations of mutant SOD proteins occur *in vivo*. Niwa *et al.* (15) reported that Dorfin, a RING finger-type ubiquitin-protein isopeptide ligase (E3) ubiquitinates the FALS mutant SODs but not wild-type Cu/Zn-SOD, suggesting that FALS mutant SODs have a unique structure that can be recognized by Dorfin. We reported previously that FALS mutant SODs are more susceptible to glycation or fructation (16) and that they form aggregates at a higher rate than the wild-type SOD, when incubated in the presence of copper ions (4). These data also

* This work was supported by a grant from The Amyotrophic Lateral Sclerosis Association (United States), "Health and Labour Sciences Research Grants and Research on Measures for Intractable Diseases" from the Ministry of Health and Welfare Japan, by The Japan Foundation for Aging and Health, by the 21st Century Center of Excellence program from the Ministry of Education, Culture, Sports, Science, and Technology of Japan, and in part by a Hitech Research Center grant from the Ministry of Education, Science, and Culture of Japan, and the Japan Foundation for Applied Enzymology. The costs of publication of this article were defrayed in part by the payment of page charges. This article must therefore be hereby marked "*advertisement*" in accordance with 18 U.S.C. Section 1734 solely to indicate this fact.

|| To whom all correspondence should be addressed: Dept. of Biochemistry, Osaka University Medical School & Graduate School of Medicine, 2-2 Yamadaoka, Suita, Osaka 565-0871, Japan. Tel.: 81-6-6879-3420; Fax: 81-6-6879-3429; E-mail: proftani@biochem.med.osaka-u.ac.jp.

[1] The abbreviations used are: ALS, amyotrophic lateral sclerosis; PBS, phosphate-buffered saline; DTT, dithiothreitol; 2-ME, 2-mercaptoethanol; ELISA, enzyme-linked immunosorbent assay; DNP, dinitrophenyl; SOD, superoxide dismutase; HPLC, high pressure liquid chromatography; FALS, familial amyotrophic lateral sclerosis; mAbs, monoclonal antibodies; WT, wild type; DNBS, 2,4-dinitrobenzenesulfonyl chloride; E3, ubiquitin-protein isopeptide ligase.

[2] N. Fujiwara, Y. Miyamoto, M. Takahashi, K. Suzuki, and N. Taniguchi, unpublished data.

indicate that FALS mutant SODs are susceptible to conformational changes. Inclusion bodies or aggregates that are immunoreactive to Cu/Zn-SOD were also observed in motor neurons and astrocytes of mice expressing mutant *SOD1*, as well as in human ALS cases linked to *SOD1* (17, 18). It has been reported recently that purified FALS mutant SODs also have a propensity to aggregate or to form amyloid-like fibrils (19–22). Therefore, it is possible that the pathology of FALS associated with mutant SODs may also involve aggregate formation and the degeneration of neuronal cells analogous to other neurodegenerative disorders such as Alzheimer's, Parkinson's, and Huntington's diseases, prion encephalopathies, and cystic fibrosis. Although it is generally thought that aggregation and amyloid formation require a conformational transition in a polypeptide chain from a native form to an improperly folded or mis-folded conformation in these diseases, the molecular basis of this remains unclear (23).

A monoclonal antibody (mAb) is a good tool for detecting structural differences and conformational changes in local areas within a protein molecule. A conformational transition of the prion protein has been detected by various mAbs (24–26). The pH-dependent conformational transition of the Alzheimer β-amyloid peptide was monitored by their mAbs (27). Inhibition of the fibrillar aggregation of the Alzheimer β-amyloid peptide (28) and inhibition of prion transmission (29) have also been reported, based on the use of mAbs.

The findings in the present study show that unfolded FALS mutant SODs show a lower immunoreactivity against three mAbs, compared with unfolded wild-type Cu/Zn-SOD in Western blots and ELISA. The epitope for all the mAbs was determined to be located in the Greek key loop VI. These data suggest that the denatured forms in this local area might well be different between wild-type and FALS mutant SODs because variations in recognition by the mAbs may indicate structural differences at this loop. This is the first demonstration of different recognition by mAbs between wild-type and FALS mutant SODs. The use of mAbs as a microprobe promises to contribute to the clarification of the structural mechanism by which FALS mutant SODs cause ALS.

EXPERIMENTAL PROCEDURES

Antibodies—Monoclonal antibodies against human Cu/Zn-SOD, N6, and SD-G6 were purchased from Panafarm (Kumamoto, Japan) and Sigma, respectively. 5c-10 was kindly provided by Dr. Uda (Hiroshima Prefecture University). Horseradish peroxidase-conjugated rabbit anti-goat IgG and goat anti-rabbit IgG were purchased from Dako (Denmark). Horseradish peroxidase-conjugated rabbit anti-mouse IgG was obtained from Promega. Picotan/picotein rabbit anti-DNP (IgG) was purchased from Cosmobio (Japan).

Cell Culture and Expression of Wild-type and Mutated Cu/Zn-SOD in Mammalian Cells—Neuro2a, a murine neuroblastoma cell line, was maintained in Dulbecco's modified Eagle's medium containing 100 units/ml penicillin and 100 μg/ml streptomycin supplemented with 10% heat-inactivated fetal bovine serum (Invitrogen) at 37 °C under an atmosphere of 95% air and 5% CO_2. Cells were transfected with the following wild-type and mutated SOD1 cDNAs transiently by Lipofectamine 2000, according to the manufacturer's instructions. The culturing of *Spodoptera frugiperda* (Sf21) cells and manipulations of the baculovirus were performed according to the procedures described by Piwnica-Worms (30). Sf21 cells were maintained in Grace's medium containing 3.3 mg/ml yeastolate, 3.3 mg/ml lactalbumin hydrolysate, and 50 μg/ml gentamycin supplemented with 10% heat-inactivated fetal bovine serum at 27 °C.

Mutagenesis and Construction of Plasmids—Point mutations were introduced into the human *SOD1* cDNA in Bluescript SK(+) using the overlap extension PCR mutagenesis procedure (31). The wild-type and mutant cDNAs were transferred into the *pcDNA3.1* mammalian expression vector and pVL1393 baculovirus expression vector between the BamHI and NotI sites. These constructs were confirmed by an automated DNA sequencing (Applied Biosystems model 310).

Western Blot Analysis—Proteins were subjected to SDS-PAGE and then transferred to a nitrocellulose membrane under semi-dry conditions by means of a Trans-blot (Bio-Rad). After blocking by incubation with 4% skim milk in Tris-buffered saline (20 mM Tris-HCl, pH 8.0, 0.15 M NaCl (TBS)) for 12 h at 4 °C, the membrane was incubated with a goat polyclonal antibody or monoclonal antibodies against human Cu/Zn-SOD (1000 ng/ml) in Tris-buffered saline containing 0.05% Tween 20 (TBS-T) and containing 1% skim milk for 2 h at room temperature. After washing with TBS-T, the membrane was incubated with peroxidase-conjugated rabbit anti-goat IgG (diluted 1:5000 in TBS-T containing 1% skim milk) or rabbit anti-mouse IgG (diluted 1:5000 in TBS-T containing 1% skim milk) for 2 h. After washing, the chemiluminescence method using an ECL kit (Amersham Biosciences) was employed to detect the peroxidase activity.

Overproduction and Purification of Wild-type and Mutant Cu/Zn-SOD Proteins—For the overproduction of Cu/Zn-SODs by the baculovirus/insect cells system, the wild-type cDNA and mutant cDNAs were ligated into the baculovirus transfer vector pVL1393 (Invitrogen) and cotransfected with BaculoGold (Pharmingen) into Sf21 cells using Lipofectin (Invitrogen). 0.5 mM $CuCl_2$ and 0.5 mM $ZnCl_2$ were added directly to the medium after viral infection. Purification of SOD proteins that were overproduced in Sf21 cells was carried out essentially as described previously (16) with minor modifications. $1–4 \times 10^8$ infected Sf21 cells were harvested and washed with PBS(−) and stored at −20 °C until used. The cells were homogenized in buffer A (2.5 mM potassium phosphate, pH 7.4) containing protein inhibitor mixture without EDTA (Roche Applied Science) and centrifuged at 100,000 × *g* for 30 min. The supernatant was applied to a DE52 cellulose column. After washing with buffer A, the bound proteins were eluted with a linear gradient of potassium phosphate from 2.5 to 200 mM. Fractions containing SOD protein were dialyzed on a PD10 column with buffer B (10 mM potassium phosphate, pH 7.4). The fractions were applied to a MonoQ-Sepharose column (Amersham Biosciences). After washing with buffer B, the bound proteins were eluted with a linear gradient of KCl (0–100 mM) in buffer B. Fractions containing SOD protein were dialyzed on a PD10 column with buffer C (10 mM potassium phosphate, pH 6.8) and applied to a hydroxyapatite type I column (Bio-Rad) to eliminate the minor contaminated proteins. After washing with buffer C, the bound proteins were eluted with a linear gradient of potassium phosphate from 10 to 300 mM. Fractions containing SOD protein were dialyzed on a PD10 column with 50 mM sodium bicarbonate, pH 9.6, and concentrated by Microcon YM-10 (Millipore). The MonoQ-Sepharose column and the hydroxyapatite column chromatography works were performed using AKTA Explorer 10S (Amersham Biosciences). The purity of SOD proteins was more than 99%, as judged by SDS-PAGE.

ELISA—Purified Cu/Zn-SOD proteins (0.25 mg/ml), with and without denaturing treatments in coating buffer (50 mM sodium bicarbonate, pH 9.6), were diluted to 1 μg/ml with coating buffer. 100 μl of the samples were added to each well of 96-well microplates (Maxisorp, Nunc), incubated overnight at 4 °C, washed three times with PBS containing 0.01% Tween 20 (PBS-T), and then blocked for 2 h at room temperature with 1% BSA in PBS. The plates were then washed three times with PBS-T, and 100 μl of monoclonal and goat polyclonal anti-human Cu/Zn-SOD antibodies (desired dilution in PBS-T) was added, followed by incubation for 1 h at room temperature. The plates were washed three times with PBS-T, and 100 μl of horseradish peroxidase-conjugated anti-mouse IgG (diluted 1:5000 in PBS-T) for monoclonal antibodies, anti-goat IgG (diluted 1:5000 in PBS-T) for a goat polyclonal antibody, or anti-rabbit IgG (diluted 1:5000 in PBS-T) for a rabbit polyclonal antibody was added and incubated for 1 h at room temperature. After washing five times with PBS-T, the plates were developed using 100 μl of *o*-phenylenediamine dihydrochloride solution, and the reaction was stopped with 25 μl of 2 M HCl. The absorbance of each well was determined at 490 nm with an Immunoreader NJ 200 (Intermed).

Preparation of DNP-SODs and Its ELISA—Preparation of DNP-SODs was performed according to a previous report by Little and Eisen (32) and the manufacturer's protocol of Picotan/picotein rabbit anti-DNP with minor modifications. Briefly, purified Cu/Zn-SOD proteins (0.25 mg/ml) were mixed with an equal volume of 2,4-dinitrobenzenesulfonyl chloride (DNBS) (1 mg/ml) in 0.5 M Na_2CO_3, pH 11.5, which had been incubated for 2 h at 37 °C, and diluted to various concentrations (0.05–1 μg/ml) in coating buffer. 100 μl of the samples were added to each well of 96-well microplates and incubated overnight at 4 °C. After washing, Picotan/picotein rabbit anti-DNP in PBS-T was directly added to the wells without a blocking step. The other steps were performed according to the method described above.

CD Analyses—Purified Cu/Zn-SOD proteins with and without denaturing treatments in coating buffer were subjected to CD spectral measurement using a Jasco J-720 spectropolarimeter (Jasco, Japan).

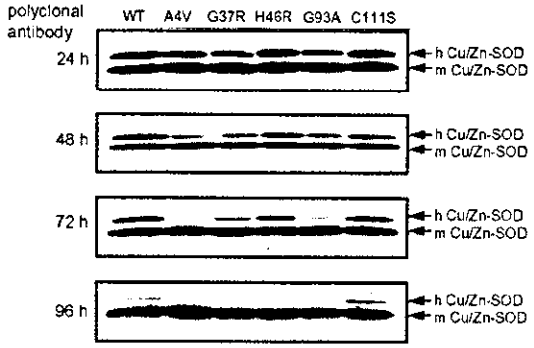

FIG. 1. **Estimation of wild-type and mutant Cu/Zn-SODs expressed in Neuro2a cells by Western blot analyses.** Two μg of mutant *SOD1* cDNAs as well as the wild-type *SOD1* cDNA were transiently transfected into Neuro2a cells by Lipofectamine. The cells were collected 24, 48, 72, and 96 h after transfection and dissolved in TNE buffer (50 mM Tris-HCl containing 1% Nonidet P-40 and 0.1 mM EDTA and protease inhibitor mixture (Roche Applied Science), pH 7.4) for 30 min on ice. After centrifugation (15,000 rpm) for 30 min, the proteins in the supernatant (20 μg) were subjected to SDS-PAGE. Human (*h*) and mouse (*m*) Cu/Zn-SODs in Neuro2a cells were detected by Western blot analyses using a polyclonal antibody.

The secondary structure was monitored over the wavelength range of 200–250 nm using a 0.1-cm path length cuvette at 25 °C. Eight scans were averaged for each sample; the averaged blank spectra of detergents dissolved into the same buffer solutions were subtracted. The CD data were expressed as mean residue ellipticity [θ] (degree cm^2/dmol). The protein concentrations under the CD measurements were 15 μM.

Epitope Mapping—0.5 mg of WT and A4V proteins were incubated at 0.25 mg/ml in 50 mM Tris-HCl, pH 8.6, containing 5 mM DTT, 7 M guanidine HCl, and 10 mM EDTA at 37 °C for 2 h. The free sulfhydryls were carboxymethylated by adding iodoacetic acid in the dark at room temperature for 30 min. After dialysis on a PD10 column with 50 mM Tris-HCl, pH 9.0, the proteins were digested with 0.25% (w/w) lysyl endopeptidase (Wako Pure Chemicals) at 37 °C for 16 h. The resulting peptides were applied to a reverse phase HPLC (AKTA Explorer 10S) at a flow rate of 1 ml/min on a Sephacryl peptide C18 column (4.6 × 250 mm, Amersham Biosciences). The peptides were separated by a linear gradient of 2–50% acetonitrile containing 0.05% trifluoroacetic acid. Peptides were detected by their absorbance at 215 nm. The peaks were subjected to mass spectrometry, amino acid sequencing, and ELISA. For the ELISA, the separated peptides or synthesized peptides were diluted with PBS(−), added to 96-well plates, and incubated for 2 h at room temperature. After washing, the first antibodies (mAbs) in PBS-T were directly added to the wells without a blocking step. The other steps were performed according to the method described above. Synthesized peptides were purchased from Sigma Genosys.

Protein Assay—Protein concentrations of crude samples were determined by using a protein assay kit (Bio-Rad) with bovine serum albumin as a standard. Purified Cu/Zn-SOD protein concentrations were estimated using a dimeric molar extinction at 280 nm of 10,800 M^{-1} cm^{-1} (33).

RESULTS

Typical FALS Mutant SODs Are Susceptible to Degradation in Neuro2a Cells—Mutant SOD1 cDNAs, A4V, G37R, H46R, G93A, and C111S were obtained using wild-type (WT) human SOD1 cDNA. The mutant C111S is not found in FALS, and Ser-111 is conserved in Cu/Zn-SOD in other mammalian species except for humans. It has also been reported that C111S is more thermally stable than the wild type (34, 35). Therefore, it would be expected that C111S does not cause ALS and can be used as a second control (wild type).

These mutant cDNAs, as well as the wild-type cDNA, were transiently transfected into Neuro2a cells. As shown in Fig. 1, although all human Cu/Zn-SOD proteins expressed the similar levels 24 h after transfection, A4V, G37R, and G93A were degraded more rapidly than H46R 48 h after transfection. The stability of the C111S protein was comparable with the wild type (WT), and both were more stable than the H46R protein.

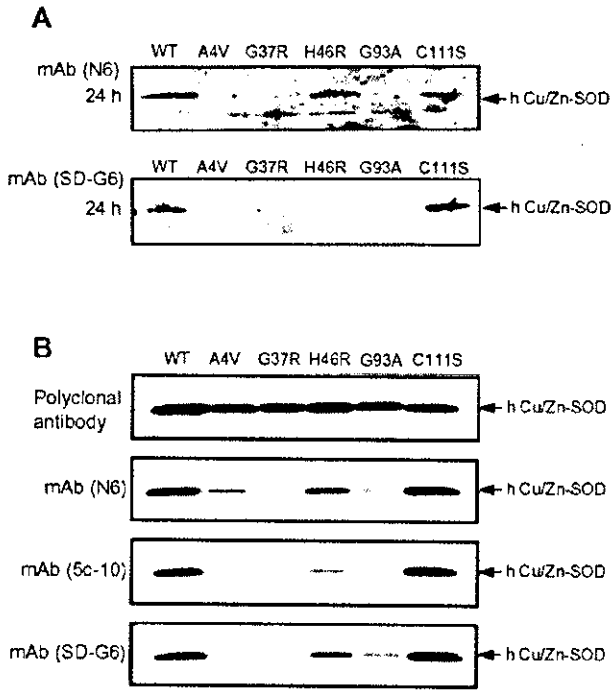

FIG. 2. **Western blot analyses of wild-type and mutant SODs detected by monoclonal antibodies.** *A*, human (*h*) Cu/Zn-SOD expressed in Neuro2a cells at 24 h after the transfection was detected by Western blot analyses using monoclonal antibodies. *B*, 30 ng of purified wild-type and mutant SODs were subjected to SDS-PAGE and were detected by Western blotting using monoclonal antibodies. Each nitrocellulose membrane, after reacting with the monoclonal antibodies, was de-probed by treatment with stripping buffer and re-incubated with a polyclonal antibody, and representative data are shown.

Endogenous mouse Cu/Zn-SOD was unchanged through the period of this observation. The addition of MG132, proteasome inhibitor, 24 h after transfection restored the protein levels of A4V, G37R, and G93A in a concentration-dependent manner (data not shown), which is consistent with previous studies (13, 14). In addition, Ratovitski *et al.* (36) have reported that H46R has longer half-life than other FALS mutant SODs in cells by 35-S pulse-chase. We have also obtained similar results that the half-lives of A4V, G37R, and G93A were shorter than H46R (data not shown). Therefore, Fig. 1 suggests that FALS mutant SODs have the propensity to be degraded in the proteasome and that H46R is longer lived than other FALS mutant SODs in cells.

Typical FALS Mutant SODs Are Barely Detected by Monoclonal Antibodies in Western Blot Analyses—We used monoclonal antibodies against human Cu/Zn-SOD (mAbs N6 and SD-G6) to detect expressed human Cu/Zn-SOD proteins in the cell lysate 24 h after transfection. As shown in Fig. 2*A*, WT and C111S were detected by both mAbs, and H46R was detected by mAb N6 slightly. However, A4V, G37R, and G93A were not detected by both mAbs (Fig. 2*A*), even though all proteins were detected at the same level by a polyclonal antibody (Fig. 1, *24 h*).

To analyze further in detail the lowered reactivity of the FALS mutant proteins with these mAbs, purified Cu/Zn-SOD proteins were subjected to Western blot analyses. As shown in Fig. 2*B*, typical FALS mutant SODs, A4V, G37R, and G93A, were scarcely detected by these mAbs, as well as by a third monoclonal antibody, mAb 5c-10. In contrast, H46R was detected by all mAbs to a greater extent than the other FALS mutant SODs, and C111S and WT reacted much more strongly with all mAbs. Each of the nitrocellulose membranes after

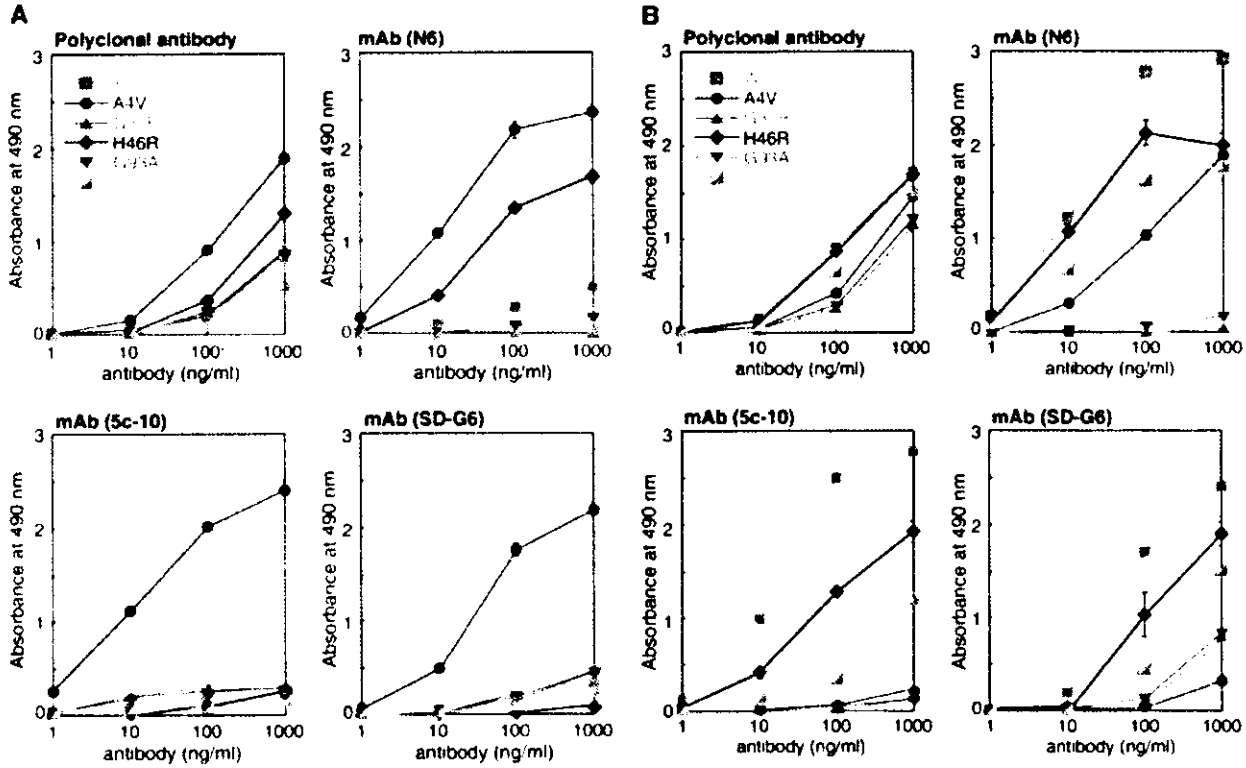

FIG. 3. **ELISA for native SODs and SODs treated the same way as in Western blot analyses.** Purified wild-type and mutant SODs with and without denaturing treatments were diluted to 1 μg/ml in coating buffer (50 mM sodium bicarbonate, pH 9.6). 100 μl of the samples were added to each well of 96-well microplates. The proteins were detected by various concentrations of mAbs and a polyclonal antibody. Data are presented as the means ± S.D. of triplicate experiments. *A*, ELISA for native wild-type and mutant SODs. *B*, ELISA for wild-type and mutant SODs treated the same way as in Western blot analyses.

reacting with the mAbs was de-probed by treatment with a stripping buffer (80 mM Tris-HCl, pH 6.8, containing 2.5% SDS, 1% 2-ME) and re-incubated with a polyclonal antibody. Representative results show that the same amounts of Cu/Zn-SOD proteins are present on the membrane. These results clearly show that typical FALS mutant SODs are barely recognized by the monoclonal antibodies in Western blot analyses despite having only one amino acid replacement.

ELISA for Denatured SODs Showed Results Similar to Western Blotting, although ELISA for Native SODs Did Not—We next examined the reactivity of the purified Cu/Zn-SOD proteins with these mAbs by means of ELISA. Unexpectedly, mAbs 5c-10 and SD-G6 recognized native A4V much stronger than other proteins, and mAb N6 recognized native A4V and H46R strongly (Fig. 3*A*), which is inconsistent with the Western blot results. Thus we performed ELISA for proteins after the treatments in the same manner in Western blotting. The SOD proteins were boiled with 2% 2-ME and 2% SDS for 5 min, diluted with coating buffer (50 mM $NaHCO_3$, pH 9.6) by 200-fold, and then subjected to ELISA. As shown in Fig. 3*B*, the treated WT, H46R, and C111S reacted with all the mAbs much more strongly than typical FALS mutant SODs. The reactivity of A4V to these mAbs was drastically decreased by this treatment. All of the treated proteins had almost the same reactivity with the polyclonal antibody. These results were very similar to the results obtained in the Western blot analyses.

All Epitopes of mAbs N6, 5c-10, and SD-G6 Are Located in the Greek Key Loop VI—The question arises as to which region of the human Cu/Zn-SOD is recognized by these monoclonal antibodies. Because there is no map of their epitopes, we performed epitope mapping for these mAbs, N6, 5c-10, and SD-G6. WT was digested with lysyl endopeptidase, and the digest was fractionated by HPLC on a Sephacryl C18 column (Fig. 4*A*). Although three peptides, 1–3, 4–9, and 129–136 were lost, the peptides corresponding to nine peaks from 1 to 9 were identified as residues 71–75, 123–128, 24–30, 76–91, 71–91, 31–36, and137–153, a mixture of 10–23, 37–70, and 92–122, respectively, as shown in Fig. 4*B*, by amino acid sequencing and mass spectrometry analyses. These peptides were diluted 10-fold with PBS(−) and subjected to ELISA. Only one peptide in peak 9, which corresponds to residues 92–122, reacted with all the mAbs (Fig. 4*C*). On the other hand, the polyclonal antibody reacted with peptides in peaks 5 and 7–9. The ELISA of peptides from digested A4V also showed the same results. To further identify the epitope for each mAb, the synthesized peptides were subjected to ELISA. As shown in Fig. 4*D* (*a* and *b*), peptide 102–116 reacted strongly with all the mAbs and the polyclonal antibody. Moreover, because residues 102–114 and 103–116 did not react with all the mAbs and the polyclonal antibody (Fig. 4*D* (c)), we conclude that epitopes of these mAbs are located within residues 102–115. These results clearly indicate that Ser-102 and Arg-115 are essential for binding to all the mAbs and the polyclonal antibody. Epitopes of the mAbs and polyclonal antibody may be composed of Ser-102 and Arg-115 and some residues between Val-103 and Gly-114. The residues 102–115 corresponds to Greek key loop VI between β-sheet 4f (residues 94–101) and β-sheet 7g (residues 116–120) in the tertiary structure of human Cu/Zn-SOD (Fig. 4*E*, *red line*). It is interesting to note that the epitopes of all mAbs are located in the same region even though they were obtained from different sources, suggesting that this loop may be a strong antigenic region in Cu/Zn-SOD. However, epitopes of the three mAbs are not identical and have different characters. N6 reacts with native A4V and H46R strongly

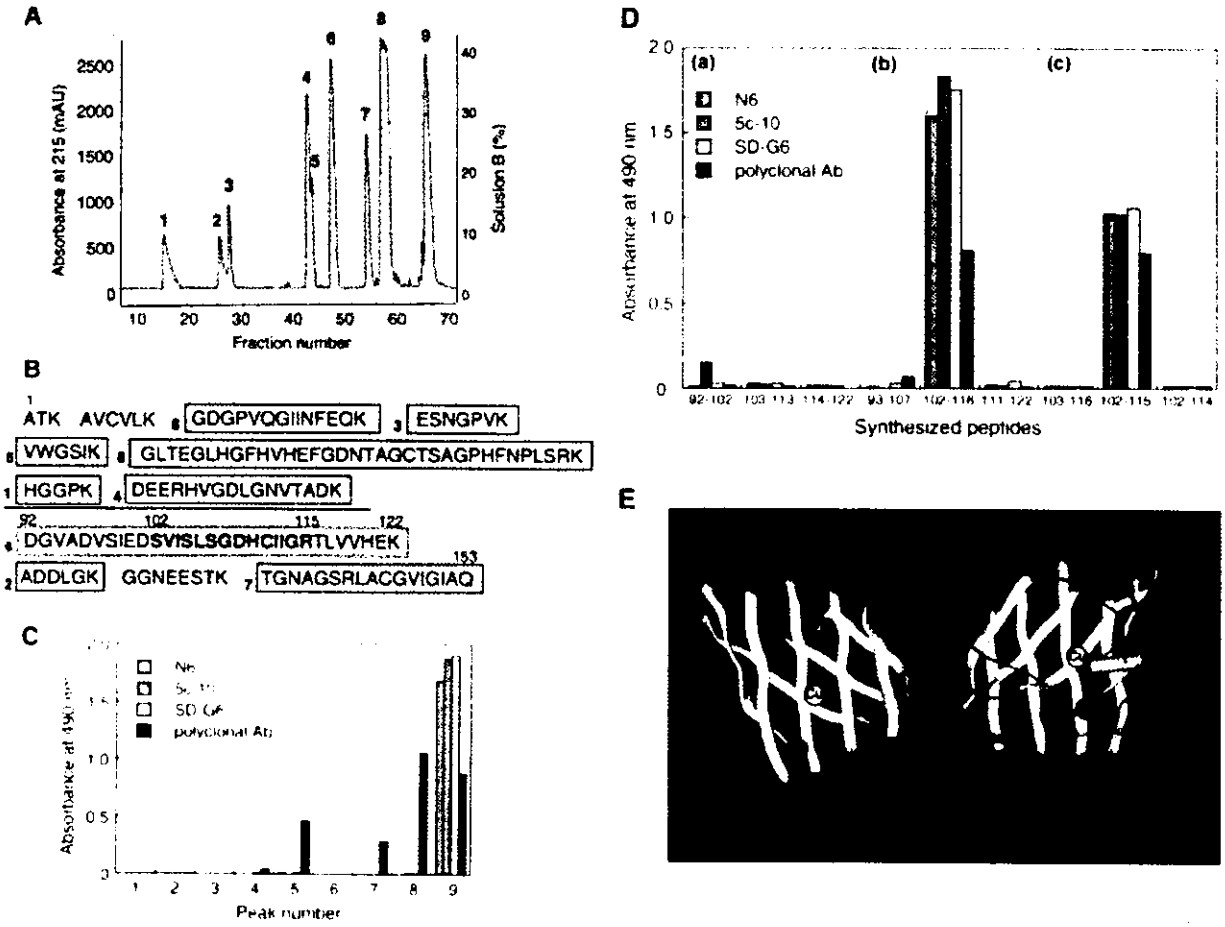

FIG. 4. **Epitope mapping of monoclonal antibodies.** *A*, wild-type SOD was digested with lysyl endopeptidase, and the digest was fractionated by HPLC using a Sephacryl C18 column. *B*, peptide mapping of human Cu/Zn-SOD. *Numbers beside* the *boxes* and *numbers above* the *amino acids* show the peak number in *A* and amino acid residue number, respectively. *C*, ELISA for the separated peptides. *D*, ELISA for synthesized peptides. Peak 9 (92–122) was divided into three peptides. *a*, each peptide consists of 11 or 9 amino acids. *b*, each peptide consists of 15 or 12 amino acids. *c*, peptides from which one or two amino acids were deleted (102–116) (*b*). *E*, epitope of the mAbs was indicated as *red lines* on the tertiary structure of A4V Cu/Zn-SOD (Protein Data Bank code 1N19).

(Fig. 3*A*) and does not react with native and denatured G37R well (Figs. 5–7), even at higher concentrations (data not shown). 5c-10 and SD-G6 recognize native A4V much stronger than other mutant SODs (Fig. 3*A*) and does not react with native H46R well.

DTT Treatment Causes Clear Differences in Immunoreactivity against mAbs between Wild-type-like Proteins and FALS Mutant Cu/Zn-SOD Proteins—Because SDS-PAGE and Western blot analyses includes a reduction with 2-ME, denaturation with SDS, and heating, we investigated the influence of each unfolding treatment on the immunoreactivity of these SOD proteins against mAbs. These SOD proteins were first treated with various concentrations of DTT in the coating buffer for 40 min and then subjected to ELISA. As shown in Fig. 5, the immunoreactivities of A4V, G37R, and G93A against all mAbs decreased after treatment with DTT at concentrations above 1 mM. On the other hand, the immunoreactivities of WT, C111S, and H46R toward all the mAbs increased at the same concentration of DTT. These data suggest that the denaturation by DTT causes clear opposite tendencies between typical FALS mutant SODs (A4V, G37R, and G93A) and wild-type like proteins (WT, C111S, and H46R), and may contribute to the differences of the recognition by mAbs in Western blot analyses. The rationale for including H46R in this group is described under the "Discussion."

SDS Treatment Affects the Immunoreactivity of SODs against mAbs—The effect of SDS treatment on reactivity against the mAbs was also monitored. SOD proteins were treated with various concentrations of SDS for 40 min, diluted 200-fold with the coating buffer, and then subjected to ELISA. As shown in Fig. 6, the immunoreactivity of both WT and mutant proteins against mAb 5c-10 and mAb SD-G6 decreased after incubation with 0.01–0.1% SDS. The reactivity of WT, C111S against 5c-10 increased only after incubation with 2% SDS. On the other hand, the reactivity of WT, C111S, and H46R against mAb N6 was increased after incubation with 1–2% SDS, whereas the reactivity of the typical FALS mutants (A4V, G37R, and G93A) decreased against all the mAbs in an SDS concentration-dependent manner.

Heat Treatment also Affects the Immunoreactivity of SODs against mAbs—Finally, the SOD proteins were incubated at various temperatures in coating buffer for 5 min by using thermal circler (Takara Bio), diluted 200-fold with the coating buffer, and then subjected to ELISA. As shown in Fig. 7, the immunoreactivity of FALS mutant SODs toward all mAbs decreased with increasing treatment temperature until 70 °C. However, the reactivity of WT and C111S against mAb N6 was drastically increased at 80 and 90 °C, respectively. The reactivity of H46R against N6 but not 5c-10 or SD-G6 was also maintained at higher temperatures. The reactivity

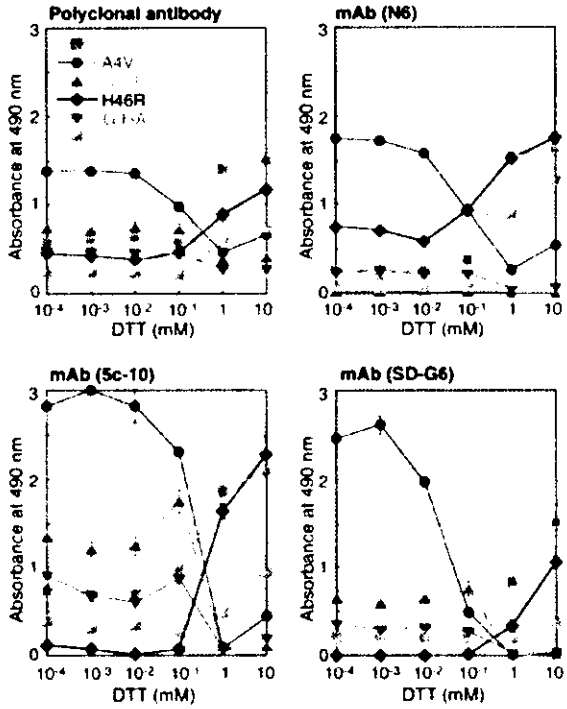

FIG. 5. **Effects of DTT treatment on immunoreactivities of the SODs to monoclonal and polyclonal antibodies.** Purified wild-type and mutant SODs were treated with various concentrations of DTT for 40 min at room temperature and diluted to 1 μg/ml in coating buffer (50 mM sodium bicarbonate, pH 9.6). 100 ng of proteins were coated on an ELISA plate and reacted with the monoclonal or polyclonal antibodies indicated in the figures. Data are presented as the means ± S.D. of triplicate experiments.

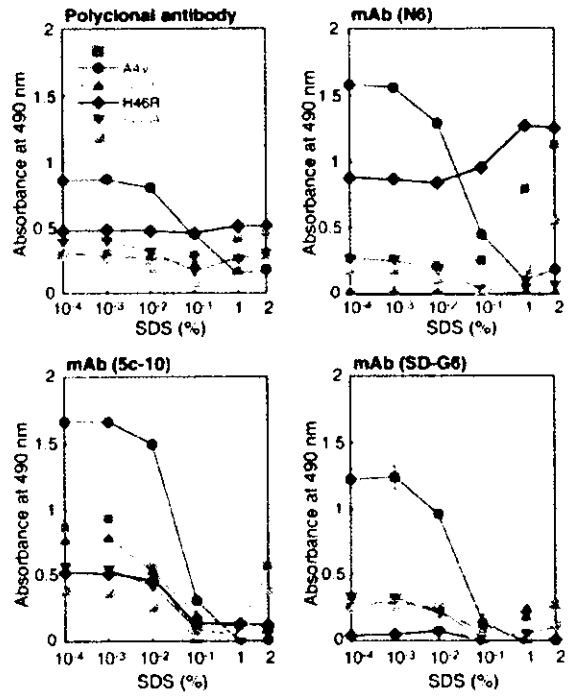

FIG. 6. **Effects of SDS treatment on immunoreactivities of the SODs to monoclonal and polyclonal antibodies.** Purified wild-type and mutant SODs were treated with various concentrations of SDS for 40 min at room temperature and diluted to 1 μg/ml in the coating buffer. 100 ng of proteins were coated into the ELISA plate and were reacted with monoclonal or polyclonal antibodies indicated in the figures. Data are presented as the means ± S.D. of triplicate experiments.

of all the SODs against SD-G6 decreased with increasing treatment temperature.

The Different Immunorecognition by mAbs between Wild-type and FALS Mutant SODs Is Not Due to a Different Binding Efficiency to ELISA Plate—A question may arise as to whether the different recognition by mAbs on ELISA (Figs. 5–7) is because of a differential coating efficiency between WT and mutant SODs on the ELISA plate or a different mAbs recognition itself. However, the protein levels on the plate were too low to be measured by authentic protein assay. Stable dinitrophenylated (DNP) protein is easily obtained by incubation with DNBS in alkaline pH solution (32). Because Picotan/picotein rabbit anti-DNP can react with the DNP proteins of the order of picogram, but not free DNP, we used this system to examine the coating efficiency. Purified SODs were treated with DNBS, diluted to various concentrations (0.05–1 μg/ml) in coating buffer, and coated on the ELISA plates. As shown in Fig. 8*A*, Picotan/picotein rabbit anti-DNP detected all DNP-SODs in the same degree, although the reaction with DNP-C111S was slightly lower. On the other hand, mAb N6 reacted with DNP-C111S strongly and with DNP-WT and DNP-A4V moderately (Fig. 8*B*), even though mAb N6 recognized native A4V and H46R strongly (Fig. 3*A*). To examine further whether the dinitrophenylation of SODs affects the immunorecognition by mAb N6 or not, SODs were treated with the same conditions in the absence of DNBS and detected by mAb N6 (Fig. 8*C*). The similar results in Fig. 8, *B* and *C*, indicate that the dinitrophenylation of SODs does not affect immunoreactivity of mAb N6. The treatment at 37 °C in alkaline solution would lead a partial denaturation of SODs. These data could exclude the possibility that a differential coating efficiency between WT and mutant SODs on the ELISA plate causes the different ELISA signal.

CD Analyses Showed That FALS Mutant SODs, Especially H46R and A4V, Are Susceptible to Denaturation by DTT, SDS, and Heat Treatment—The effects of these unfolding treatments, such as DTT, SDS, and heat treatment, on the secondary (whole) structure of SOD proteins were assessed by CD measurements. The spectra of all of the SODs were almost the same for the native state, although H46R showed a slightly different spectrum (Fig. 9*A*). These SODs, in coating buffer, were reduced with various concentrations of DTT for 40 min and then subjected to CD analysis. 0.1 mM DTT began to induce small denaturation in H46R, A4V, and G93A (Fig. 9*B*), and all the FALS mutant SODs, except WT and C111S, were denatured by 1 mM DTT treatment (Fig. 9*C*). The reduced FALS mutant SODs showed a larger negative band at about 202 nm, an increased negative ellipticity from 220 to 240 nm, and a less negative band in the 215 nm region, which indicates an increased random coil/unordered structure and a decreased β-structure.

We next examined the effect of SDS on the structure of these proteins. As shown in Fig. 9*D*, treatment with 2% SDS caused a loss of secondary structure in only H46R and A4V but not in WT, C111S, G37R, and G93A. The structure of H46R and A4V began to change by treatment with SDS at concentrations above 0.05% (data not shown). The CD profiles showed more helical conformation as reported for monomeric *Escherichia coli* Cu/Zn-SOD treated with SDS at concentrations above 10% (37), which are quite different from the form produced by reduction with DTT (Fig. 9*C*). These data indicate that only H46R and A4V are quite sensitive to SDS and that a propensity toward denaturation by SDS is not common among FALS mutant SODs.

Finally, all SODs that were boiled in the coating buffer for 5 min were subjected to CD analyses. As shown in Fig. 9*E*, the

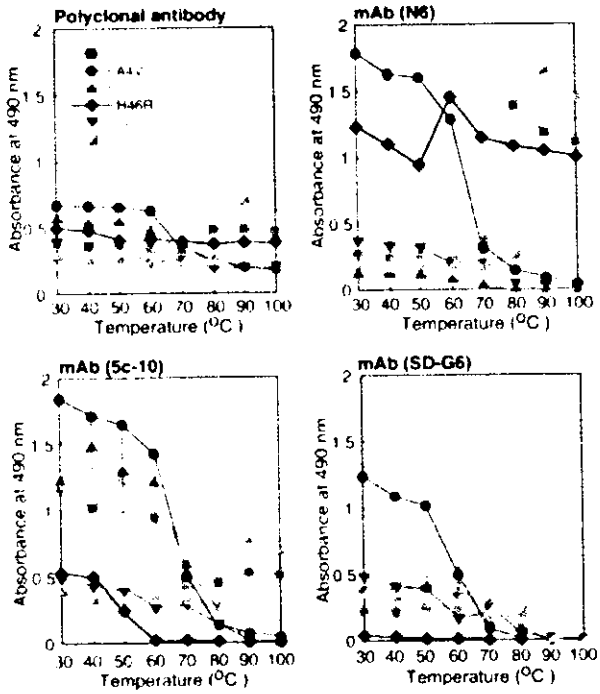

FIG. 7. **Effects of heating on immunoreactivities of the SODs to monoclonal and polyclonal antibodies.** Purified wild-type and mutant SODs were treated at various temperatures for 5 min and diluted to 1 μg/ml with coating buffer. 100 ng of proteins were coated into ELISA plate and reacted with monoclonal or polyclonal antibodies indicated in the figures. Data are presented as the means ± S.D. of triplicate experiments.

CD spectra of all proteins were identical, even though differences in immunoreactivity between wild-type SOD and FALS mutant SODs, when treated at over 80 or 90 °C, were detected by ELISA for mAb N6 and mAb 5c-10 (Fig. 7). Because the CD spectra patterns also showed lower ellipticity from 220 to 240 nm as well as the reduced FALS mutant SODs (Fig. 9*C*), we monitored the transition curves of these proteins at 25–70 °C at a wavelength of 230 nm. H46R and A4V began to denature at a lower temperature, indicating that both are much more thermolabile than the other SODs (Fig. 9*F*). These results indicate that FALS mutant SODs, especially H46R and A4V, are susceptible to denaturation by DTT, SDS, and heat treatment.

DISCUSSION

Although there is some evidence to show that the FALS mutant SODs have a toxic gain of function, the mechanism responsible of this pathology is unknown. Finding the differences of properties between wild-type and FALS mutant SODs and the common characteristics of FALS mutant SODs will give clues to solve the etiology of FALS. The findings here show that typical FALS mutant SODs, but not wild-type SOD, are barely recognized by three monoclonal antibodies in Western blot analyses and ELISA after denaturation, which were in parallel with their degree of increased biological turnover of FALS mutants. Because the epitopes of the three mAbs were mapped within residues 102–115 (Greek key loop VI), variations in recognition by the mAbs may indicate different conformations in this loop. We have observed that the conformation of the peptide 92–122 (Fig. 4*C*, *peak 9*), including the Greek key loop VI, is changeable depending on the solvents, such as water, saline (150 mM NaCl), and PBS, by CD measurements and that the peptide reacts with mAb N6 only when solved in PBS on ELISA.[2] Preliminary one-dimensional ^{1}H NMR spectroscopy of the peptide 92–122 was also performed by a Bruker DRX-800 spectrometer. Most of the NMR peaks derived from the aromatic and amide ^{1}H spins were observed in a narrow spectra range from 7.9 to 8.7 ppm. In addition, peaks from the aliphatic spins were crowded and were separated into several groups. These features of the ^{1}H spectra also suggest that the peptide 92–122 takes neither a typical secondary structure nor a rigid conformation.[3]

Shipp *et al.* (38) have reported that comparison of dynamic properties between G93A and wild-type by NMR spectroscopy showed that G93A exhibits a higher mobility than wild type, particularly in loop III (residues 37–40), which is another short Greek key loop, and loop V (residues 89–93). The increased mobility of the longer Greek key loop VI (residues 102–115) was not described in the NMR study. However, Greek key loop VI may also have property to move easily, because loop regions normally display greater mobility than residues involved in secondary structural elements (38). Because the NMR study needs enough stability for analyzing all residues of the polypeptide at room temperature, the Greek key loop VI in G93A may be stable at the native state. On the other hand, the NMR study of A4V failed because degradation was found from the NMR spectra just a few days after purification (38).

The Greek key loop VI contributes to the stability of Cu/Zn-SOD. In particular, Leu-106 and Ile-113 in the Greek key loop act to stabilize the β-barrel and dimer interface. The Leu-106 side chain points toward the protein core to create a "cork," which stabilizes the β-barrel structure through hydrophobic interactions (39). The mutation from Cys-111 to Ser-111 (C111S) has an increased conformational stability resulting, in part, from the stronger side chain to main chain hydrogen bonds from the O$^\gamma$ of Ser-111 to the N of Ile-113 and the O of Leu-106 in the Greek key loop (10). By contrast, the crystallographic structure of A4V showed that a mutation from Ala-4 to Val-4 causes the movement of the Leu-106 to cork out of the barrel, even though this A4V protein has the mutation from Cys-111 to Ser-111 (40). The higher immunoreactivity of the mAbs against native A4V may indicate this loose shape of the Greek key loop VI. In the case of WT or C111S, the loop may change to the loose shape only after denaturation. Further studies on which shape of the Greek key loop VI reacts with each mAb will be needed.

Reduction by DTT caused the largest differences in recognition by mAbs between wild-type and FALS mutant SODs. As shown in Fig. 5, the immunoreactivities of A4V, G37R, and G93A against all mAbs were drastically decreased when treated with DTT at concentrations above 1 mM, whereas those of WT, C111S, and H46R increased oppositely at the same concentration of DTT. CD analyses also showed that FALS mutant SODs are much more unstable to DTT treatment than WT and C111S (Fig. 9*C*). Tiwari and Hayword (41) reported that, in the presence of disulfide-reducing agents, FALS mutant SODs were more susceptible than WT to aberrant migration during partially denaturing SDS-PAGE and to proteolytic digestion. A conserved internal disulfide bond between Cys-57 and Cys-146 also contributes to the stability of Cu/Zn-SOD. Cys-57 is located in the longest loop IV containing residues 49–84 between β-sheet 6d and β-sheet 5e, which comprises part of the dimer interface and forms the zinc-binding site. Cys-146 is located in β-sheet 8h containing residues 145–152. A part in the β-sheet 8h is hydrogen bonding with Gly-114 and Arg-115 in the Greek key loop VI (9). Therefore, the presence of DTT in coating buffer, pH 9.6, would induce the cleavage of the

[3] T. Ikegami and N. Fujiwara, unpublished data.

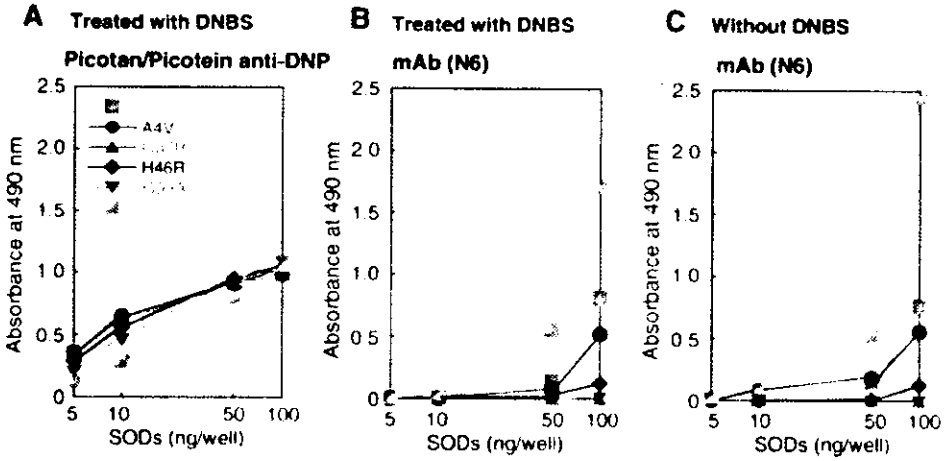

FIG. 8. **Determination of coating efficiency of wild-type and mutant SODs to ELISA plate by using DNP-SODs and Picotan/picotein rabbit anti-DNP.** DNP-SODs were coated on the ELISA plate and reacted with Picotan/picotein rabbit anti-DNP (*A*) and with mAb N6 (*B*). *C*, SODs were treated with the same conditions of dinitrophenylation in the absence of DNBS and detected by mAb N6. Data are presented as the means ± S.D. of triplicate experiments.

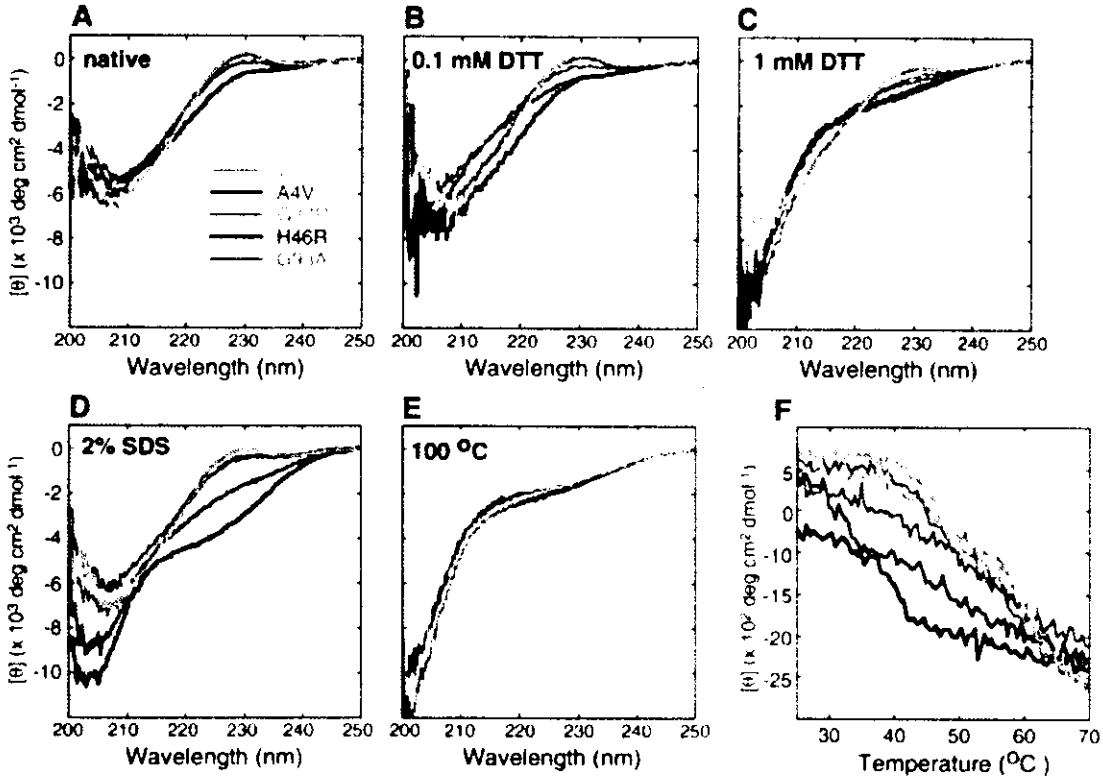

FIG. 9. **Effects of DTT, SDS, and heating on far-UV CD spectra of the Cu/Zn-SOD proteins.** *A*, CD spectra of native wild-type and mutant SODs in coating buffer. *B*, CD spectra of wild-type and mutant SODs treated with 0.1 mM DTT in coating buffer for 40 min. *C*, CD spectra of wild-type and mutant SODs treated with 1 mM DTT in coating buffer for 40 min. *D*, CD spectra of wild-type and mutant SODs treated with 2% SDS in coating buffer for 40 min. *E*, CD spectra of wild-type and mutant SODs boiled in coating buffer for 5 min. *F*, transitions in the CD ellipticities of wild-type and mutant SODs at 25–70 °C monitored at a wavelength of 230 nm.

disulfide bond and cause disorder in loop IV, the β-sheet 8h, and the structure of the Greek key loop VI. However, even though the mutation sites are far from the Greek key loop VI and each mutation site is different, the question of why it is clearly different in terms of immunoreactivity against mAbs between wild-type Cu/Zn-SOD-like proteins (WT, C111S, and H46R) and typical FALS mutant SODs (A4V, G37R, and G93A) after DTT treatment remains unanswered. The reason for why H46R is included in the wild-type like SOD group is discussed below.

Because His-46 is one of the copper-ligand amino acids in Cu/Zn-SOD, the mutant enzyme, H46R, contains no copper and thus is SOD-inactive (4). However, the possibility must be considered that H46R is more stable than other typical FALS mutant SODs. Among FALS patients, the clinical progression is quite different from the mutations in the *SOD1* gene. For H46R patients, the progression is extremely slow, with a mean survival of 16.8 years (42). In contrast, the mean survival of G93A cases in one report was 2.2 years (43). Recently, Nagai *et*

al. (44) established an H46R rat and a G93A rat. Even though the H46R SOD protein level in the H46R rat was much higher than that in the G93A rat, both the onset and the rate of progression of the disease in the H46R rat were much slower than those for the G93A rat (44). We also observed that H46R has a longer half-life than the other FALS mutants (Fig. 1) (36). Moreover, Niwa *et al.* (15) reported that ubiquitination of H46R by Dorfin, which is the likely ubiquitin ligase for FALS mutant SODs, was lower than other FALS mutant SODs. Recently, Miyazaki *et al.* (45) reported that NEDL1, a novel HECT-type ubiquitin ligase, also ubiquitinates FALS mutants and that the degree of ubiquitination of mutant SODs was dependent on the disease severity of FALS (A4V > G93A > H46R). These results also indicate that H46R is much more stable than other FALS mutant SODs *in vivo*. In contrast, the recombinant H46R protein is quite sensitive to DTT, SDS, and heat treatment (Fig. 9). Several papers (41, 46) have also reported that H46R is less stable than other FALS mutants *in vitro*. Most interestingly, the immunoreactivities of H46R against the mAbs in Western blot and ELISA were similar to that of WT or C111S (Figs. 2, 3, and 5–7). Therefore, local conformational changes monitored with mAbs will be useful for understanding the discrepancy between the instability of the H46R protein *in vitro* and the slower clinical progression of H46R patients.

There is accumulating evidence that FALS mutant SODs also tend to form aggregates under the destabilizing conditions (19–22), similar to other neurodegenerative disorders such as Alzheimer's, Parkinson's, Huntington's, and prion diseases. It is generally thought that aggregation or amyloid formation requires a conformational transition in a polypeptide chain from a native form to a mis-folded conformation in these diseases. In the case of prion disease, the conformational conversion of a normal α-helical rich cellular prion protein (PrP^c) to an abnormal and insoluble β-sheet rich form (PrP^{sc}) is a key event in the pathogenesis (47). The structural rearrangement in the central portion (residues 90–120) in the PrP^c is associated with the conversion to the infectious conformer (25). Thus the peculiar, subtle conformational change in the Greek key loop in FALS mutant SODs may also serve as a trigger for aggregation or amyloid formation. Moreover, if small change in FALS mutant SODs are recognized by ubiquitin ligase specific for FALS mutant SOD proteins, such as Dorfin or NEDL1, FALS mutant SODs would undergo a more rapid degradation in cells. To determine the significance of the alteration in the Greek key loop for FALS mutant SODs, further studies using various mAbs recognizing other regions and other mutant SODs are needed.

In the present study, we found different recognition by mAbs between wild-type and FALS mutant SODs under the denatured conditions, which suggests that different conformations are induced around the Greek key loop during the unfolding process. This new approach using mAbs will contribute to a better understanding of the molecular mechanism of the conformational perturbation of FALS mutant proteins, and may be of value in the development of a diagnosis and therapeutic agents for use in treating FALS.

Acknowledgments—We thank Dr. Taizou Uda (Hiroshima Prefecture University) for kindly providing mAb 5c-10. We are grateful to Dr. Tomitake Tsukihara (Institute of Protein Research, Osaka University) for helpful comments.

REFERENCES

1. Deng, H. X., Hentati, A., Tainer, J. A., Zafar, I., Cayabyab, A., Hung, W. Y., Getzoff, E. D., Hu, P., Herzfeldt, B., Roos, R. P., Warner, C., Deng, G., Soriano, E., Smyth, C., Parge, H. E., Ahmed, A., Roses, A. D., Hallewell, R. A., Pericak-Vance, M. A., and Siddique, T. (1993) *Science* **261,** 1047–1051
2. Rosen, D. R., Siddique, T., Patterson, D., Figlewicz, D. A., Sapp, P., Hentati, A., Donaldson, D., Goto, J., O'Regan, J. P., Deng, H. X., Rahmani, Z., Krizus, A., McKenna-Yasek, D., Cayabyab, A., Gaston, S. M., Berger, R., Tanzi, R. E., Halperin, J. J., Herzfeldt, B., Van den Bergh, R., Hung, W. Y., Bird, T., Deng, G., Mulder, D. W., Smyth, C., Laing, N. G., Soriano, E., Pericak-Vance, M. A., Hains, J., Rouleau, G. A., Gusella, J. S., Horvitz, H. R., and Brown, R. H., Jr. (1993) *Nature* **362,** 59–62
3. Valentine, J. S., and Hart, P. J. (2003) *Proc. Natl. Acad. Sci. U. S. A.* **100,** 3617–3622
4. Okado-Matsumoto, A., Myint, T., Fujii, J., and Taniguchi, N. (2002) *Free Radic. Res.* **33,** 65–73
5. Gurney, M. E., Pu, H., Chiu, A. Y., Dal Canto, M. C., Polchow, C. Y., Alexander, D. D., Caliendo, J., Hentati, A., Kwon, Y. W., Deng, H. X., Chen, W., Zhai, P., Sufit, R. L., and Siddique, T. (1994) *Science* **264,** 1772–1775
6. Ripps, M. E., Huntley, G. W., Hof, P. R., Morrison, J. H., and Gordon, J. W. (1995) *Proc. Natl. Acad. Sci. U. S. A.* **92,** 689–693
7. Reaume, A. G., Elliott, J. L., Hoffman, E. K., Kowall, N. W., Ferrante, R. J., Siwek, D. F., Wilcox, H. M., Flood, D. G., Beal, M. F., Brown, R. H., Jr., Scott, R. W., and Snider, W. D. (1996) *Nat. Genet.* **13,** 43–47
8. Julien, J. P. (2001) *Cell* **104,** 581–591
9. Tainer, J. A., Getzoff, E. D., Beem, K. M., Richardson, J. S., and Richardson, D. C. (1982) *J. Mol. Biol.* **160,** 181–217
10. Parge, H. E., Hallewell, R. A., and Tainer, J. A. (1992) *Proc. Natl. Acad. Sci. U. S. A.* **89,** 6109–6113
11. Lindberg, M. J., Tibell, L., and Oliveberg, M. (2002) *Proc. Natl. Acad. Sci. U. S. A.* **99,** 16607–16612
12. Hayward, L. J., Rodriguez, J. A., Kim, J. W., Tiwari, A., Goto, J. J., Cabelli, D. E., Valentine, J. S., and Brown, R. H., Jr. (2002) *J. Biol. Chem.* **277,** 15923–15931
13. Borchelt, D. R., Lee, M. K., Slunt, H. S., Guarnieri, M., Xu, Z. S., Wong, P. C., Brown, R. H., Jr., Price, D. L., Sisodia, S. S., and Cleveland, D. W. (1994) *Proc. Natl. Acad. Sci. U. S. A.* **91,** 8292–8296
14. Hoffman, E. K., Wilcox, H. M., Scott, R. W., and Siman, R. (1996) *J. Neurol. Sci.* **139,** 15–20
15. Niwa, J., Ishigaki, S., Hishikawa, N., Yamamoto, M., Doyu, M., Murata, S., Tanaka, K., Taniguchi, N., and Sobue, G. (2002) *J. Biol. Chem.* **277,** 36793–36798
16. Takamiya, R., Takahashi, M., Myint, T., Park, Y. S., Miyazawa, N., Endo, T., Fujiwara, N., Sakiyama, H., Misonou, Y., Miyamoto, Y., Fujii, J., and Taniguchi, N. (2003) *FASEB J.* **17,** 938–940
17. Bruijn, L. I., Houseweart, M. K., Kato, S., Anderson, K. L., Anderson, S. D., Ohama, E., Reaume, A. G., Scott, R. W., and Cleveland, D. W. (1998) *Science* **281,** 1851–1854
18. Johnston, J. A., Dalton, M. J., Gurney, M. E., and Kopito, R. R. (2000) *Proc. Natl. Acad. Sci. U. S. A.* **97,** 12571–12576
19. Rakhit, R., Cunningham, P., Furtos-Matei, A., Dahan, S., Qi, X. F., Crow, J. P., Cashman, N. R., Kondejewski, L. H., and Chakrabartty, A. (2002) *J. Biol. Chem.* **277,** 46551–47556
20. Stathopulos, P. B., Rumfeldt, J. A., Scholz, G. A., Irani, R. A., Frey, H. E., Hallewell, R. A., Lepock, J. R., and Meiering, E. M. (2003) *Proc. Natl. Acad. Sci. U. S. A.* **100,** 7021–7026
21. DiDonato, M., Craig, L., Huff, M. E., Thayer, M. M., Cardoso, R. M., Kassmann, C. J., Lo, T. P., Bruns, C. K., Powers, E. T., Kelly, J. W., Getzoff, E. D., and Tainer, J. A. (2003) *J. Mol. Biol.* **332,** 601–615
22. Elam, J. S., Taylor, A. B., Strange, R., Antonyuk, S., Doucette, P. A., Rodriguez, J. A., Hasnain, S. S., Hayward, L. J., Valentine, J. S., Yeates, T. O., and Hart, P. J. (2003) *Nat. Struct. Biol.* **10,** 461–467
23. Temussi, P. A., Masino, L., and Pastore, A. (2003) *EMBO J.* **22,** 355–361
24. Peretz, D., Williamson, R. A., Matsunaga, Y., Serban, H., Pinilla, C., Bastidas, R. B., Rozenshteyn, R., James, T. L., Houghten, R. A., Cohen, F. E., Prusiner, S. B., and Burton, D. R. (1997) *J. Mol. Biol.* **273,** 614–622
25. Leclerc, E., Peretz, D., Ball, H., Sakurai, H., Legname, G., Serban, A., Prusiner, S. B., Burton, D. R., and Williamson, R. A. (2001) *EMBO J.* **20,** 1547–1554
26. Leclerc, E., Peretz, D., Ball, H., Solforosi, L., Legname, G., Safar, J., Serban, A., Prusiner, S. B., Burton, D. R., and Williamson, R. A. (2003) *J. Mol. Biol.* **326,** 475–483
27. Matsunaga, Y., Saito, N., Fujii, A., Yokotani, J., Takakura, T., Nishimura, T., Esaki, H., and Yamada, T. (2002) *Biochem. J.* **361,** 547–556
28. Solomon, B., Koppel, R., Hanan, E., and Katzav, T. (1996) *Proc. Natl. Acad. Sci. U. S. A.* **93,** 452–455
29. Peretz, D., Williamson, R. A., Kaneko, K., Vergara, J., Leclerc, E., Schmitt-Ulms, G., Mehlhorn, I. R., Legname, G., Wormald, M. R., Rudd, P. M., Dwek, R. A., Burton, D. R., and Prusiner, S. B. (2001) *Nature* **412,** 739–743
30. Piwnica-Worms, H. (1987) in *Current Protocols in Molecular Biology* (Ausubel, F. M., Brent, R., Kingston, R. E., Moore, D. D., Seidman, J. G., Smith, J. A., and Struhl, K., eds) pp. 16.8.1–16.11.7, Greene/Wiley Interscience, New York
31. Ho, S. N., Hunt, H. D., Horton, R. M., Pullen, J. K., and Pease, L. R. (1989) *Gene* **77,** 51–59
32. Little, J. R., and Eisen, H. N. (1967) in *Methods in Immunology and Immunochemistry* (William, C. A., and Chase, M. W., eds) Vol. 1, pp. 128–133, Academic Press, New York
33. Goto, J. J., Gralla, E. B., Valentine, J. S., and Cabelli, D. E. (1998) *J. Biol. Chem.* **273,** 30104–30109
34. Lepock, J. R., Frey, H. E., and Hallewell, R. A. (1990) *J. Biol. Chem.* **265,** 21612–21618
35. Hallewell, R. A., Imlay, K. C., Lee, P., Fong, N. M., Gallegos, C., Getzoff, E. D., Tainer, J. A., Cabelli, D. E., Tekamp-Olson, P., Mullenbach, G. T., and Cousens, L. S. (1991) *Biochem. Biophys. Res. Commun.* **181,** 474–480
36. Ratovitski, T., Corson, L. B., Strain, J., Wong, P., Cleveland, D. W., Culotta, V. C., and Borchelt, D. R. (1999) *Hum. Mol. Genet.* **8,** 1451–1460
37. Bozzi, M., Battistoni, A., Sette, M., Melino, S., Rotilio, G., and Paci, M. (2001) *Int. J. Biol. Macromol.* **29,** 99–105
38. Shipp, E. L., Cantini, F., Bertini, I., Valentine, J. S., and Banci, L. (2003)